

## Meso-substituted AB<sub>3</sub>-type phenothiazinyl porphyrins and their indium and zinc complexes photosensitising properties, cytotoxicity and phototoxicity on ovarian cancer cells.

Brém Balázs<sup>1</sup>, Bianca Stoean<sup>1</sup>, Éva Molnár<sup>1</sup>, Eva Fischer-Fodor<sup>2</sup>, Ovidiu Bălăcescu<sup>2</sup>, Raluca Borlan<sup>3</sup>, Monica Focsan<sup>3,4</sup>, Adriana Grozav<sup>5</sup>, Patriciu Achimaş-Cadariu<sup>2,6</sup>, Gál Emese<sup>1\*</sup>,  
Luiza Gaina<sup>1\*</sup>

<sup>1</sup> Research Center on Fundamental and Applied Heterochemistry, Faculty of Chemistry and Chemical Engineering, Babeş-Bolyai University 11 Arany Janos str., RO-400028 Cluj-Napoca, România

<sup>2</sup> Institute of Oncology “Prof. Dr. I. Chiricuta”, RO-400015 Cluj-Napoca, România

<sup>3</sup> Nanobiophotonics and Laser Microspectroscopy Center, Interdisciplinary Research Institute in Bio-Nano-Sciences, Babes-Bolyai University, 42 Treboniu Laurian Street, 400271 Cluj-Napoca, Romania

<sup>4</sup> Biomolecular Physics Department, Faculty of Physics, Babes-Bolyai University, 1 M. Kogalniceanu Street, 400084, Cluj-Napoca, Romania

<sup>5</sup> Faculty of Pharmacy, "Iuliu Hatieganu" University of Medicine and Pharmacy, Victor Babes 41, RO-400012 Cluj-Napoca, Romania

<sup>6</sup> Department of Oncological Surgery and Gynecological Oncology, “Iuliu Hatieganu” University of Medicine and Pharmacy, RO-400012 Cluj-Napoca, România

\*Correspondence: ioana.gaina@ubbcluj.ro (L.G.); Tel.: +40-264-593833

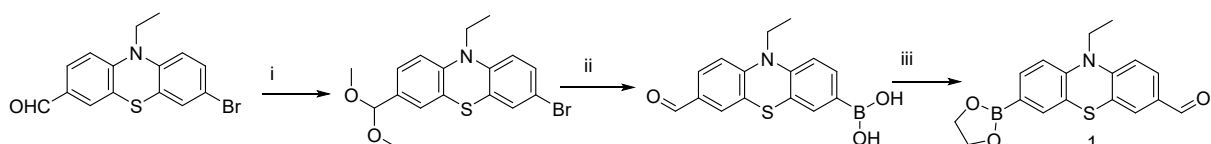
\*Correspondence: emese.gal@ubbcluj.ro (L.G.); Tel.: +40-264-593833

### Table of Content:

I. Synthesis of 7-(1,3,2-dioxaborolan-2-yl)-10-ethyl-10H-phenothiazine-3-carbaldehyde <i>comp. 1</i> .....	2
II. Spectre .....	5
Fig.S1. <sup>1</sup> H NMR of <i>comp. 2</i> , CDCl <sub>3</sub> , 400MHz .....	5
Fig.S2. <sup>13</sup> C NMR of <i>comp. 2</i> , CDCl <sub>3</sub> , 100MHz .....	5
Fig.S3. HRMS (ESI+) of <i>comp. 2</i> .....	6
Fig.S4. <sup>1</sup> H NMR of <i>comp. 2a</i> , CDCl <sub>3</sub> , 400MHz .....	6
Fig.S5. <sup>13</sup> C NMR of <i>comp. 2a</i> , CDCl <sub>3</sub> , 100MHz .....	7
Fig.S6. HRMS (ESI+) of <i>comp. 2a</i> .....	7
Fig.S7. <sup>1</sup> H NMR of <i>comp. 4</i> , CDCl <sub>3</sub> , 400MHz .....	8
Fig.S8. <sup>13</sup> C NMR of <i>comp. 4</i> , CDCl <sub>3</sub> , 100MHz .....	9
Fig.S9. HRMS (APCI+) of <i>comp. 4</i> .....	9
Fig.S10. <sup>1</sup> H NMR of <i>comp. 4a</i> , CDCl <sub>3</sub> , 400MHz .....	9
Fig.S11. <sup>13</sup> C NMR of <i>comp. 4a</i> , CDCl <sub>3</sub> , 100MHz .....	10
Fig.S12. HRMS (ESI+) of <i>comp. 4a</i> .....	10
Fig.S13. <sup>1</sup> H NMR of <i>comp. 4b</i> , CDCl <sub>3</sub> , 400MHz .....	11
Fig.S15. HRMS (ESI+) of <i>comp. 4b</i> .....	12
Fig.S16. <sup>1</sup> H NMR of <i>comp. 5a</i> , CDCl <sub>3</sub> , 400MHz .....	12

Fig.S17. <sup>13</sup> C NMR of <b>comp. 5a</b> , CDCl <sub>3</sub> , 100MHz.....	13
Fig.S18. HRMS (ESI+) of <b>comp. 5a</b> .....	13
II. Synthesis of In(III) 5,10,15,20-tetraphenyl porphyrin chloride, <b>comp. 6a</b> .....	13
Fig.S19. <sup>1</sup> H NMR of <b>comp. 6a</b> , CDCl <sub>3</sub> , 400MHz.....	14
Fig.S20. <sup>13</sup> C NMR of <b>comp. 6a</b> , CDCl <sub>3</sub> , 100MHz .....	15
Fig.S21. HRMS (APCI+) of <b>comp. 6a</b> .....	15
Fig.S22. a) normalised UV-Vis absorbance spectra of comp. <b>5</b> and <b>5a</b> in DMSO, b) normalised fluorescence emission spectra of comp. <b>5</b> and <b>5a</b> in DMSO.....	16
Fig.S23. Sigmoidal dose-response curves resulted from the depiction of survival percents relative to the untreated control (y axis) in relation to the logarithm of the compounds concentration (x axis).....	16
Table S1. The cell survival in A2780 populations treated with sublethal concentration of compounds <b>2</b> , <b>2a</b> , <b>4</b> , <b>4a</b> , <b>b</b> , <b>5</b> , <b>5a</b> , <b>6</b> , <b>6a</b> .....	17
Figure S24. Fluorescence microscopy images of A2780 cells treated with porphyrin derivatives <b>4</b> , <b>4b</b> , <b>2</b> , <b>5</b> and <b>6</b> at a final concentration of 20 μM under standard cell culture conditions (37°C, 5% CO <sub>2</sub> ), incubated for 24 (top) and 72 hours (bottom). .....	18
Figure S25. Fluorescence microscopy images of A2780 cells treated with porphyrin derivatives <b>4</b> , <b>4b</b> , <b>2</b> , <b>5</b> and <b>6</b> , in comparison with their corresponding bright field images...	18
Fig.S26. The level of nuclear factor erythroid 2-related factor 2 (Nrf-2) in A2780 cells subjected to treatment with the sublethal doses of 20μM <b>2</b> , <b>2a</b> , <b>4</b> , <b>4a</b> , <b>b</b> , <b>5</b> , <b>5a</b> , <b>6a</b> and TPP <b>6</b> , in the presence or absence of photodynamic therapy. The Nrf2 ratio was calculated against the untreated control Nrf2 values, or against the PDT-irradiated, untreated control, respectively.....	19
Fig.S27. a. -j. Significant correlations between different biologic features: cytotoxicity, metabolic reductive capacity, singlet oxygen quantum yield, reactive oxygen species (ROS) and Nrf2 expression following the A2780 cells treatment with <b>2</b> , <b>2a</b> , <b>4</b> , <b>4a</b> , <b>4b</b> , <b>5</b> , <b>5a</b> , <b>6a</b> , respectively the cells treatment with <b>2</b> , <b>2a</b> , <b>4</b> , <b>4a</b> , <b>4b</b> , <b>5</b> , <b>5a</b> , <b>6a</b> and photoradiation. ....	22
Fig.S28. Normalised spectrum of DBPF sensor degradation in the presence of compounds <b>2</b> , <b>2a</b> , <b>4</b> , <b>4a</b> , <b>b</b> , <b>5</b> , <b>5a</b> , <b>6</b> , <b>6a</b> (in DMSO).....	23
Fig. S29. The influence of the treatment on NF-κB transcription factor.....	24
Fig. S30. 72-hours follow up of the A2780 metabolic activity modulation by the compounds.....	25

### I. Synthesis of 7-(1,3,2-dioxaborolan-2-yl)-10-ethyl-10H-phenothiazine-3-carbaldehyde **comp.1**



Scheme S1. The synthesis of 7-(1,3,2-dioxaborolan-2-yl)-10-ethyl-10H-phenothiazine-3-carbaldehyde **1** starting from 7-bromo-10-ethyl-10H-phenothiazine-3-carbaldehyde

#### Synthesis of 3-bromo-7-(dimethoxymethyl)-10-ethyl-10H-phenothiazine

To the solution of 7-bromo-10-ethyl-10H-phenothiazine-3-carbaldehyde (2 g, 6 mmol) in MeOH (100 mL) was added 1.1 ml of trimethoxymethane (1.06 g, ρ=0.97 g/ml, 10 mmol) and toluene-4-sulfonic acid monohydrate (0.1 g, 0.5 mmol). The yellow solution was refluxed for 6h. The reaction mixture was allowed to cool down to room temperature and quenched with

saturated NaHCO<sub>3</sub>. To this residue, EtOAc (100 ml) was added. After separating the two layers, the aqueous layer was extracted with EtOAc (3x20 ml). The combined organic layers were dried over anhydrous MgSO<sub>4</sub>, and the solvent was removed. The resulting acid labile residue was purified by flash column chromatography (SiO<sub>2</sub>, Hexane/EtOAc = 5/1 v/v) to afford the title compound as a yellow oil. Yield: 2.2 g, 96%;

**MALDI-TOF (in DCTB):** Calcd: 379.02/381.02, Found: 379.02/381.02;

**<sup>1</sup>H-NMR (400MHz, C<sub>6</sub>D<sub>6</sub>):** δ<sub>ppm</sub> = 0.86 (t, 3H, H<sub>b</sub>), 3.11 (s, 6H, H<sub>d</sub>), 3.15 (q, 2H, H<sub>a</sub>), 5.25 (s, 1H, H<sub>c</sub>), 6.05 (d, 1H, H<sub>9</sub>, <sup>3</sup>J = 8.7 Hz), 6.44 (d, 1H, H<sub>1</sub>, <sup>3</sup>J = 8.4 Hz), 6.99 (dd, 1H, H<sub>8</sub>, <sup>3</sup>J = 6 Hz, <sup>4</sup>J = 1.4 Hz), 7.09 (d, 1H, H<sub>6</sub>, <sup>4</sup>J = 1.3 Hz), 7.31 (dd, 1H, H<sub>2</sub>, <sup>3</sup>J = 5.6 Hz, <sup>4</sup>J = 1.02 Hz), 7.39 (dd, 1H, H<sub>4</sub>, <sup>4</sup>J = 1.04 Hz);

**<sup>13</sup>C-NMR (100 MHz, C<sub>6</sub>D<sub>6</sub>):** δ<sub>ppm</sub> = 12.1 (CH<sub>3</sub>, C<sub>b</sub>), 42.5 (CH<sub>2</sub>, C<sub>a</sub>), 51.5 (CH<sub>3</sub>, C<sub>d</sub>), 101.8 (C<sub>H</sub>, C<sub>c</sub>), 114.4 (C<sub>q</sub>, C<sub>7</sub>), 114.5 (C<sub>q</sub>, C<sub>1</sub>), 115.9 (C<sub>H</sub>, C<sub>9</sub>), 123.6 (C<sub>q</sub>, C<sub>5a</sub>), 125.8 (C<sub>H</sub>, C<sub>2</sub>), 126.0 (C<sub>H</sub>, C<sub>4</sub>), 126.8 (C<sub>q</sub>, C<sub>4a</sub>), 129.5 (C<sub>H</sub>, C<sub>6</sub>, C<sub>8</sub>), 133.0 (C<sub>q</sub>, C<sub>3</sub>), 143.8 (C<sub>H</sub>, C<sub>9a</sub>), 144.4 (C<sub>q</sub>, C<sub>10a</sub>);

**IR (KBr):** ν̄(cm<sup>-1</sup>) = 2934, 2826, 1463, 1348, 1237, 1103, 1052, 804;

**UV-Vis** (CH<sub>2</sub>Cl<sub>2</sub>, λ<sub>max</sub> nm, ε): 250 (2.25·10<sup>4</sup>), 276 (2.84·10<sup>4</sup>), 388 (0.78·10<sup>4</sup>);

### ***Synthesis of (10-ethyl-7-formyl-10H-phenothiazine-3-yl)boronic acid***

To a solution of 3-bromo-7-(dimethoxymethyl)-10-ethyl-10H-phenothiazine (1.3 g, 3.42 mmol) in anhydrous THF (35 mL) was added dropwise 6.25 ml n-butyllithium (1.6 M, 10.2 mmol) at -78°C under nitrogen and the mixture was stirred for 1.5 h at -78°C. To the resulting mixture was added dropwise 1.5 ml triisopropyl borate (1.88 g, ρ=0.815 g/ml 10.2 mmol) at -78°C and the mixture was stirred for 1.5 h at -78°C and all night at room temperature. A saturated ammonium chloride aqueous solution (30 mL) was added slowly at 0°C and the organic layer was separated, washed with brine and dried with anhydrous magnesium sulfate. The solvent was evaporated under reduced pressure, and the crude product was precipitated with pentane, filtered, and washed with ice-cold CH<sub>2</sub>Cl<sub>2</sub>, to afford the title compound as a yellow powder. Yield: 0.822 g, 80%;

**MALDI-TOF (in DCTB):** Calcd: 299.07, Found: 299.08;

**<sup>1</sup>H-NMR (400MHz, Acetone-d<sub>6</sub>):** δ<sub>ppm</sub> = 1.42 (t, 3H, H<sub>b</sub>), 4.08 (q, 2H, H<sub>a</sub>), 7.06 (d, 1H, H<sub>9</sub>, <sup>3</sup>J = 8.16 Hz), 7.15 (d, 1H, H<sub>1</sub>, <sup>3</sup>J = 8.52 Hz), 7.21 (s, 2H, B(OH)<sub>2</sub>), 7.57-7.58 (m, 2H, H<sub>6</sub>, H<sub>4</sub>), 7.71 (dd, 2H, H<sub>8</sub>, H<sub>2</sub>, <sup>3</sup>J = 8.32 Hz, <sup>4</sup>J = 1.76 Hz), 9.82 (s, 1H, H<sub>3</sub>);

**<sup>13</sup>C-NMR (100 MHz, Acetone-d<sub>6</sub>):** δ<sub>ppm</sub> = 12.1 (CH<sub>3</sub>, C<sub>b</sub>), 42.0 (CH<sub>2</sub>, C<sub>a</sub>), 114.9 (C<sub>H</sub>, C<sub>9</sub>), 115.1 (C<sub>H</sub>, C<sub>1</sub>), We were not able to detect the <sup>13</sup>C signals of the *ipso*-position (C<sub>7</sub>) in CDCl<sub>3</sub> and Acetone-d<sub>6</sub> because of line broadening due to the short relaxation time and the quadrupole moment of boron-11 (I=3/2)<sup>1</sup>. 121.4 (C<sub>q</sub>, C<sub>5a</sub>), 123.9 (C<sub>q</sub>, C<sub>4a</sub>), 127.4 (C<sub>H</sub>, C<sub>6</sub>), 130.0 (C<sub>H</sub>, C<sub>8</sub>),

131.5 (C<sub>q</sub>, C<sub>3</sub>), 132.9 (C<sub>H</sub>, C<sub>4</sub>), 134.1 (C<sub>H</sub>, C<sub>2</sub>), 144.8 (C<sub>q</sub>, C<sub>9a</sub>), 149.6 (C<sub>q</sub>, C<sub>10a</sub>), 189.6 (CH, C<sub>3'</sub>);

**<sup>11</sup>B-NMR (128 MHz, Acetone-d<sub>6</sub>):** δ<sub>ppm</sub> = 28.29 (s, 1B);

**IR (KBr):**  $\bar{\nu}$ (cm<sup>-1</sup>) = 3400, 2931, 2868, 1674, 1577, 1336, 1243, 1202, 813, 740;

**Anal.** Calcd for C<sub>15</sub>H<sub>14</sub>NO<sub>3</sub>BS: C, 60.22; H, 4.72; N, 4.68; Found: C, 61.78; H, 4.95; N, 4.46;

**UV-Vis** (CH<sub>2</sub>Cl<sub>2</sub>, λ<sub>max</sub> nm, ε): 250 (1.76·10<sup>4</sup>), 286 (3.35·10<sup>4</sup>), 393 (0.78·10<sup>4</sup>);

### **Synthesis of 7-(1,3,2-dioxaborolan-2-yl)-10-ethyl-10H-phenothiazine-3-carbaldehyde (1)**

To a solution of (10-ethyl-7-formyl-10H-phenothiazin-3-yl)boronic acid (1.5 g, 5 mmol) in toluene (70 mL) was added 1.67 ml ethylene glycol (1.86 g, ρ = 1.113 g/ml, 30 mmol) and the mixture was refluxed for 12 h, a Dean-Stark trap was used to collect the eliminated water from the reaction. The *reaction mixture* was allowed to *cool down* to *room temperature*, and a saturated solution of sodium chloride (30 ml) was added to the reaction mixture. The mixture was extracted with toluene, and the extract was dried over magnesium sulfate and then concentrated to dryness. The residue underwent chromatography on silica with dichloromethane-acetone (10:1). The product was precipitated with pentane, filtered, and dried to afford the title compound as a yellow powder. Yield: 1.14 g, 70%;

**MALDI-TOF (in DCTB):** Calcd: 325.0944, Found: 325.0950;

**<sup>1</sup>H-NMR (400MHz, CDCl<sub>3</sub>):** δ<sub>ppm</sub> = 1.45 (t, 3H, H<sub>b</sub>), 3.98 (q, 2H, H<sub>a</sub>), 4.35 (s, 4H, H<sub>c</sub>), 6.88 (d, 1H, H<sub>9</sub>, <sup>3</sup>J = 8.2 Hz), 6.90 (d, 1H, H<sub>1</sub>, <sup>3</sup>J = 8.52 Hz), 7.50 (d, 1H, H<sub>6</sub>, <sup>4</sup>J = 1.4 Hz), 7.55 (d, 1H, H<sub>4</sub>, <sup>4</sup>J = 1.92 Hz), 7.58 (dd, 1H, H<sub>8</sub>, <sup>3</sup>J = 8.16 Hz, <sup>4</sup>J = 1.48 Hz), 7.62 (dd, 1H, H<sub>2</sub>, <sup>3</sup>J = 8.44 Hz, <sup>4</sup>J = 1.92 Hz), 9.78 (s, 1H, H<sub>3'</sub>);

**<sup>13</sup>C-NMR (100 MHz, CDCl<sub>3</sub>):** δ<sub>ppm</sub> = 12.9 (CH<sub>3</sub>, C<sub>b</sub>), 42.7 (CH<sub>2</sub>, C<sub>a</sub>), 66.18 (CH<sub>2</sub>, C<sub>c</sub>), 114.6 (C<sub>H</sub>, C<sub>9</sub>), 115.0 (C<sub>H</sub>, C<sub>1</sub>), We were not able to detect the <sup>13</sup>C signals of the *ipso*-position (C<sub>7</sub>) in CDCl<sub>3</sub> and Acetone-d<sub>6</sub> because of line broadening due to the short relaxation time and the quadrupole moment of boron-11 (I = 3/2)<sup>2</sup>. 121.4 (C<sub>q</sub>, C<sub>5a</sub>), 124.5 (C<sub>q</sub>, C<sub>4a</sub>), 128.4 (C<sub>H</sub>, C<sub>6</sub>), 130.1 (C<sub>H</sub>, C<sub>8</sub>), 131.3 (C<sub>q</sub>, C<sub>3</sub>), 133.9 (C<sub>H</sub>, C<sub>4</sub>), 134.7 (C<sub>H</sub>, C<sub>2</sub>), 145.8 (C<sub>q</sub>, C<sub>9a</sub>), 149.7 (C<sub>q</sub>, C<sub>10a</sub>), 190.1 (CH, C<sub>3'</sub>);

**<sup>11</sup>B-NMR (128 MHz, CDCl<sub>3</sub>):** δ<sub>ppm</sub> = 31.05 (s, 1B);

**IR (KBr):**  $\bar{\nu}$ (cm<sup>-1</sup>) = 3435, 2984, 2917, 1686, 1582, 1475, 1369, 1337, 1247, 1198, 813, 1107, 997, 949, 812, 655;

**Elemental Anal.** Calcd for C<sub>17</sub>H<sub>16</sub>NO<sub>3</sub>BS: C, 62.79; H, 4.96; N, 4.31; Found: C, 63.06; H, 4.92; N, 4.25;

**UV-Vis** (CH<sub>2</sub>Cl<sub>2</sub>, λ<sub>max</sub> nm, ε): 253 (1.90·10<sup>4</sup>), 283 (3.58·10<sup>4</sup>), 392 (0.78·10<sup>4</sup>);

## II. Spectra

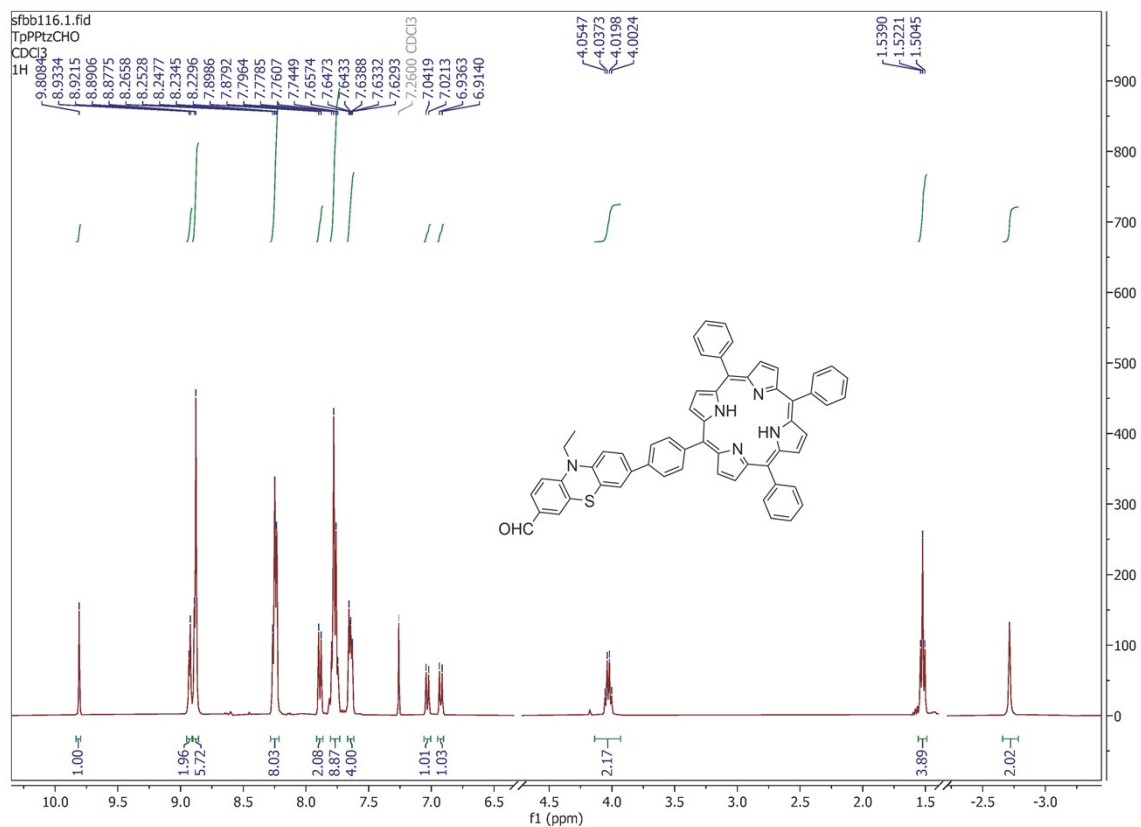


Fig.S1. <sup>1</sup>H NMR of **comp. 2**, CDCl<sub>3</sub>, 400MHz

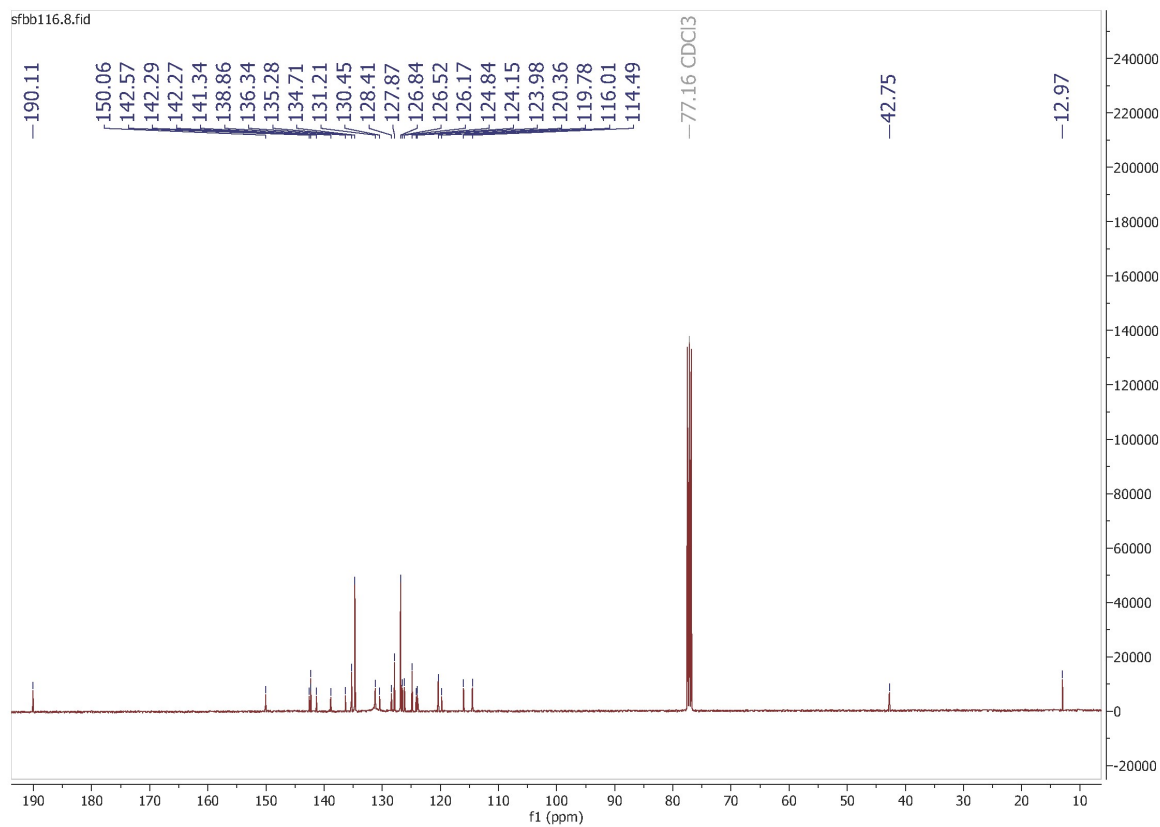


Fig.S2. <sup>13</sup>C NMR of **comp. 2**, CDCl<sub>3</sub>, 100MHz

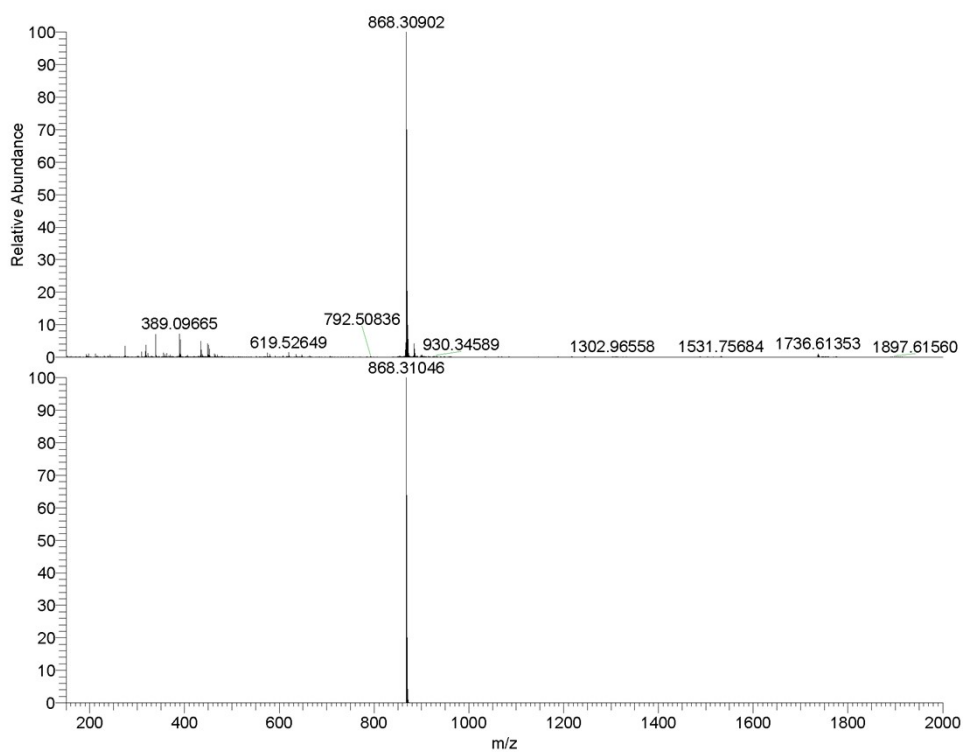


Fig.S3. HRMS (ESI+) of *comp. 2*

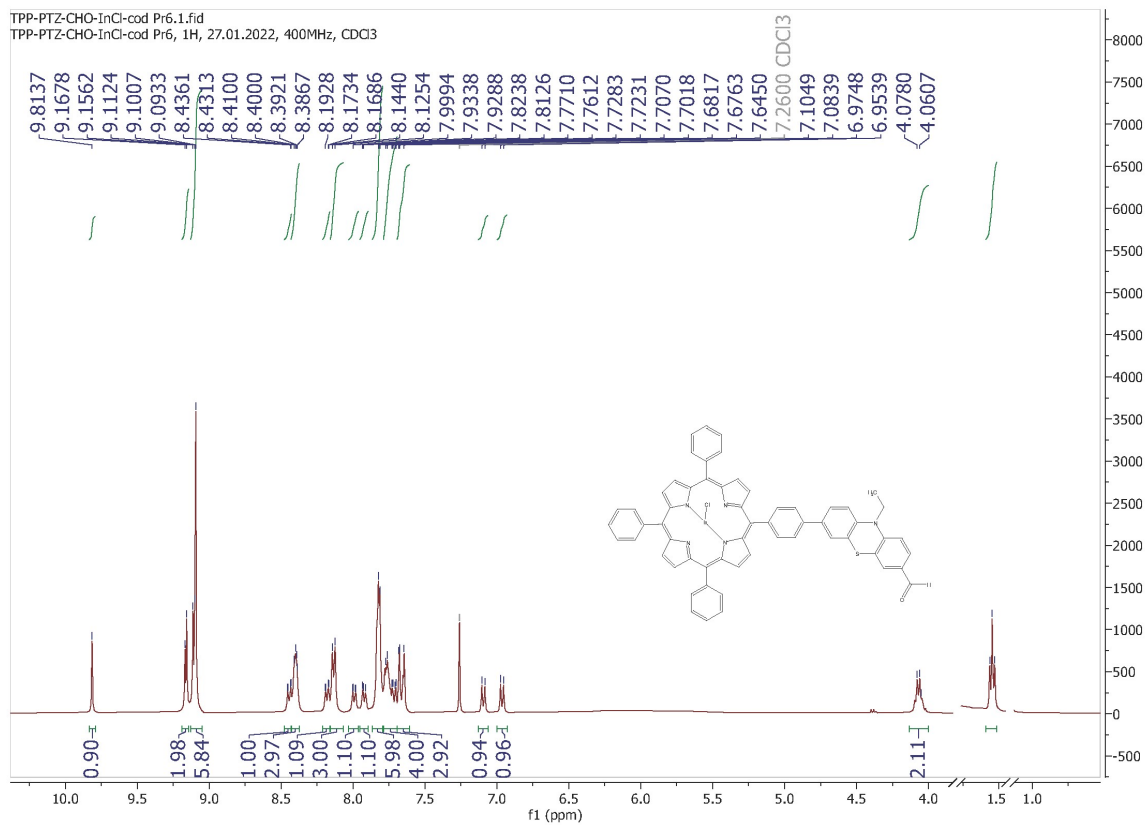


Fig.S4. <sup>1</sup>H NMR of *comp. 2a*, CDCl<sub>3</sub>, 400MHz

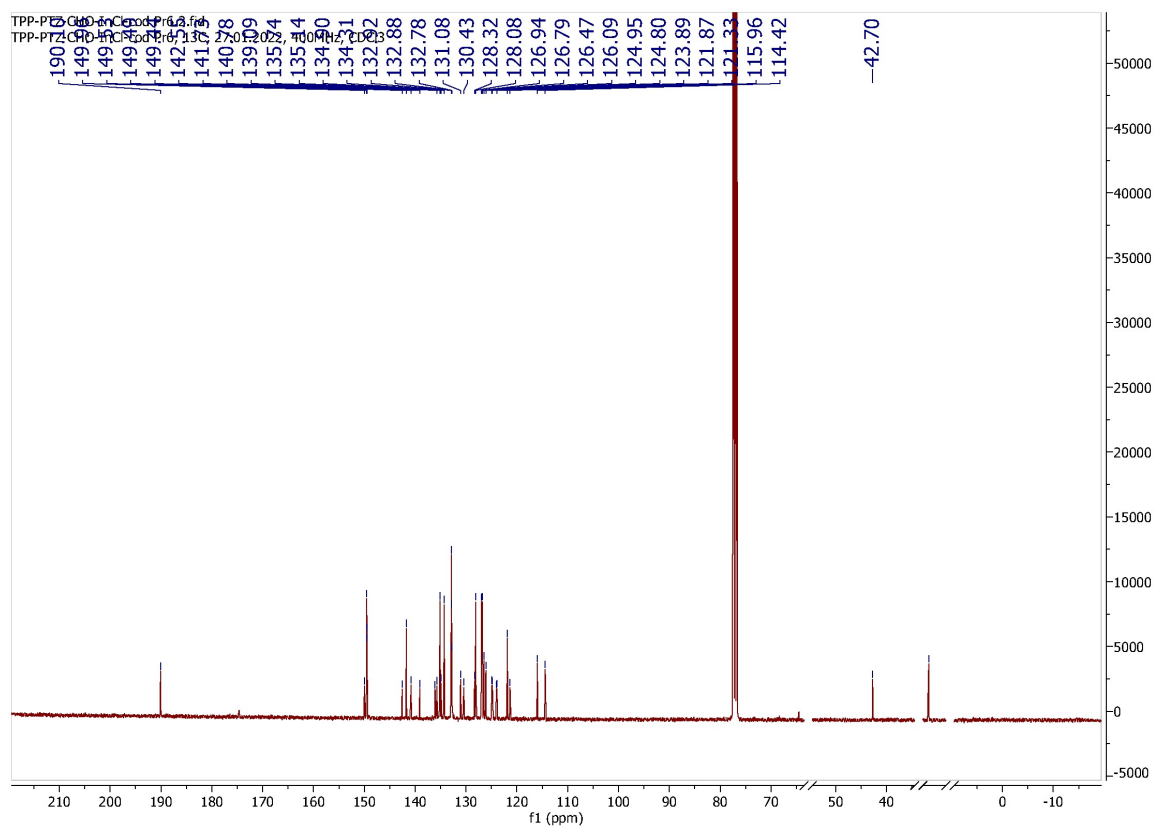


Fig.S5.  $^{13}\text{C}$  NMR of *comp. 2a*,  $\text{CDCl}_3$ , 100MHz

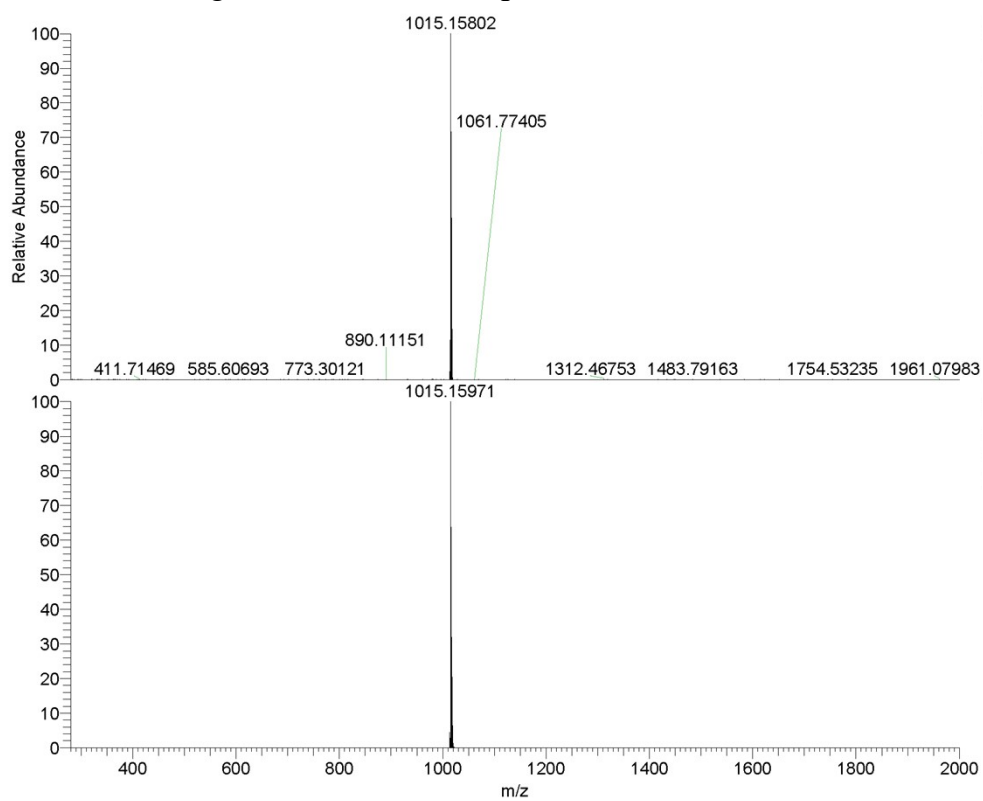


Fig.S6. HRMS (ESI+) of *comp. 2a*

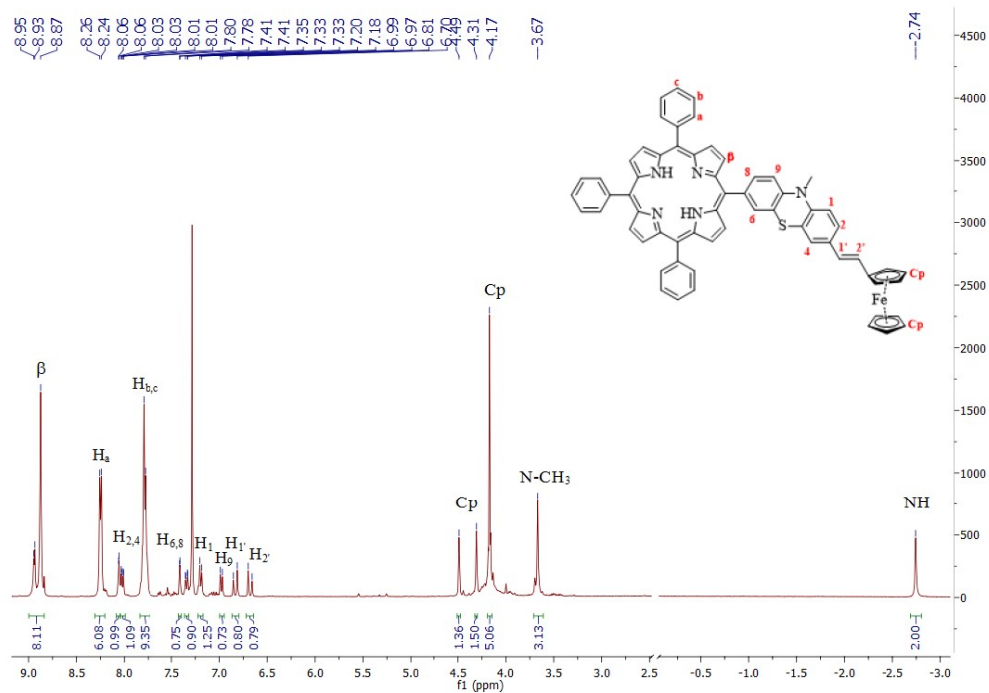


Fig.S7.  $^1\text{H}$  NMR of *comp. 4*,  $\text{CDCl}_3$ , 400MHz

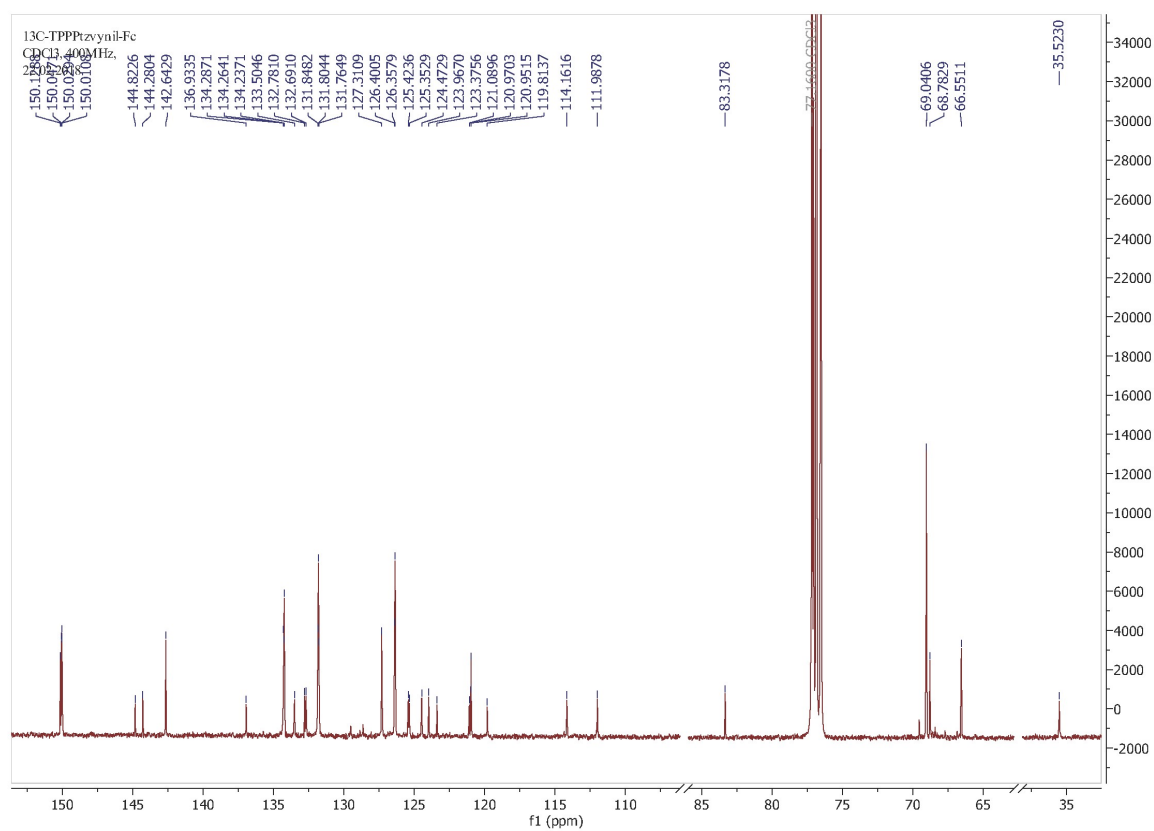


Fig.S8.  $^{13}\text{C}$  NMR of *comp. 4*,  $\text{CDCl}_3$ , 100MHz

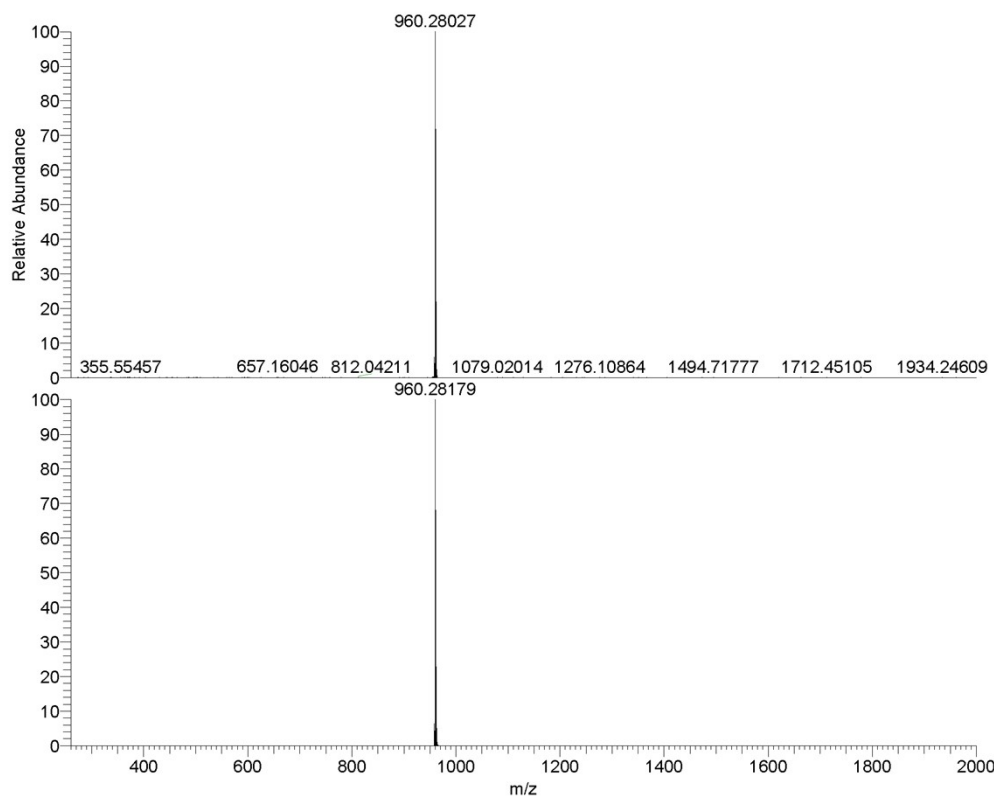


Fig.S9. HRMS (APCI+) of *comp. 4*

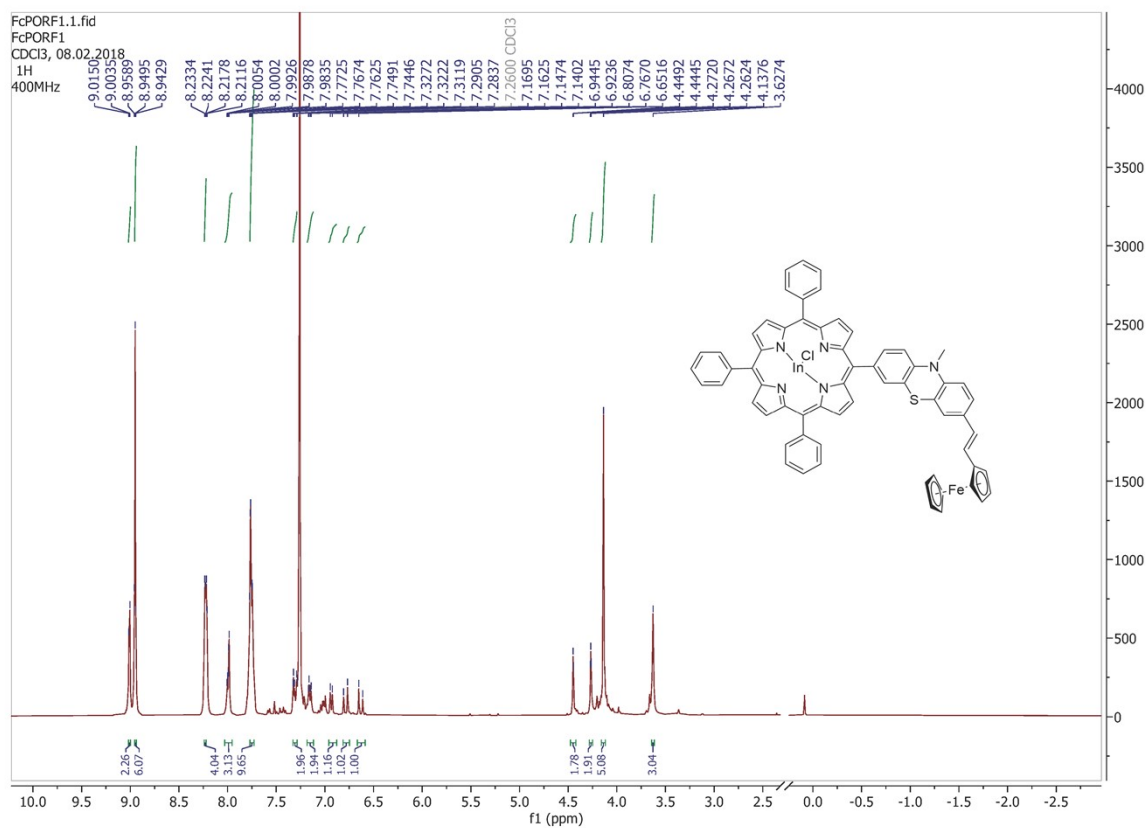


Fig.S10. <sup>1</sup>H NMR of *comp. 4a*, CDCl<sub>3</sub>, 400MHz

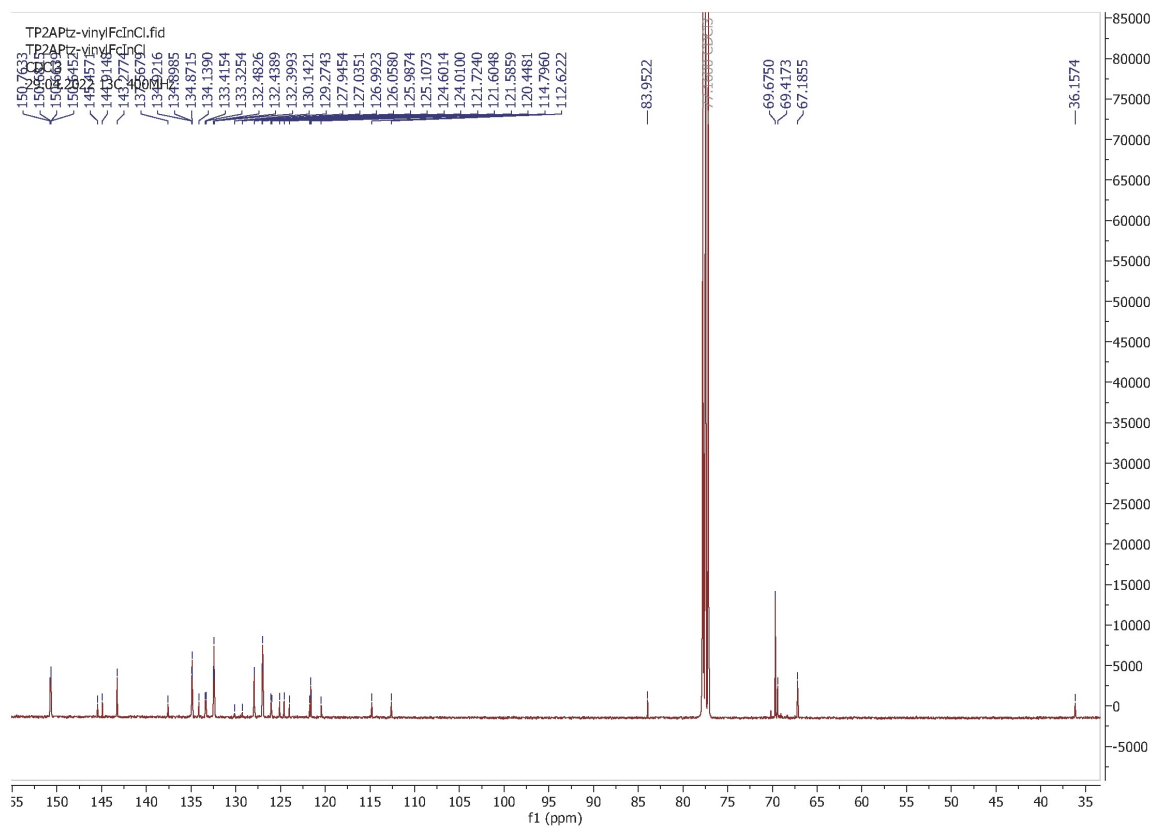


Fig.S11.  $^{13}\text{C}$  NMR of *comp. 4a*,  $\text{CDCl}_3$ , 100MHz

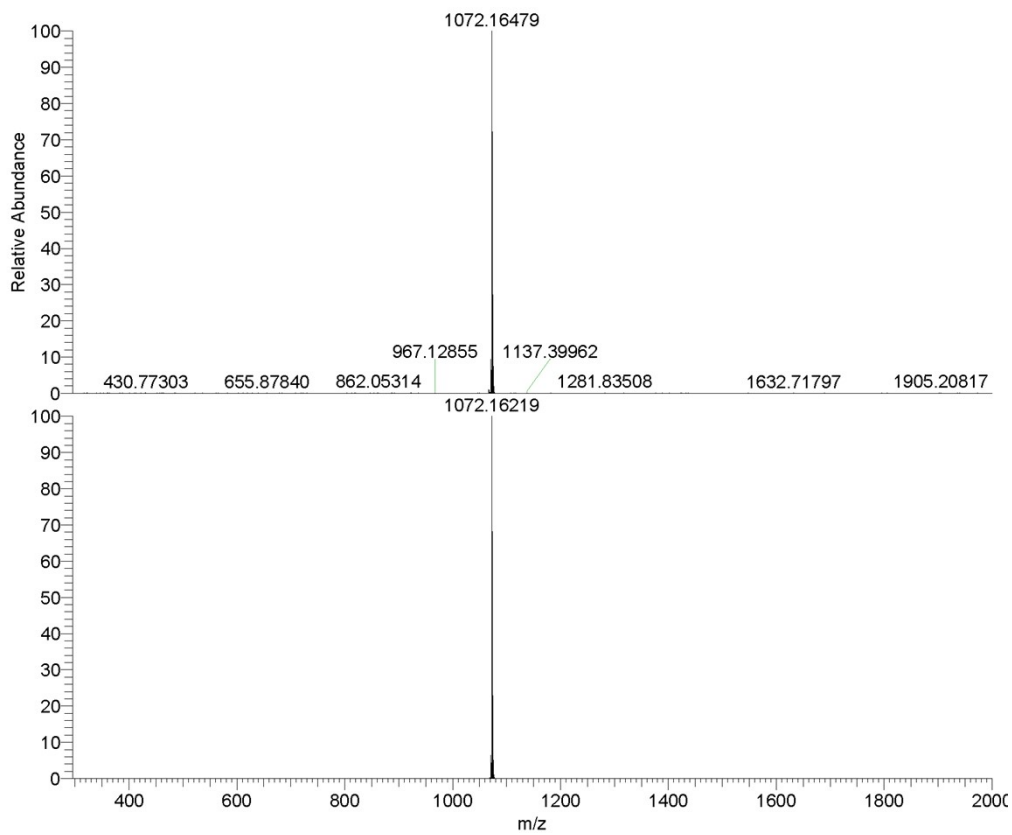
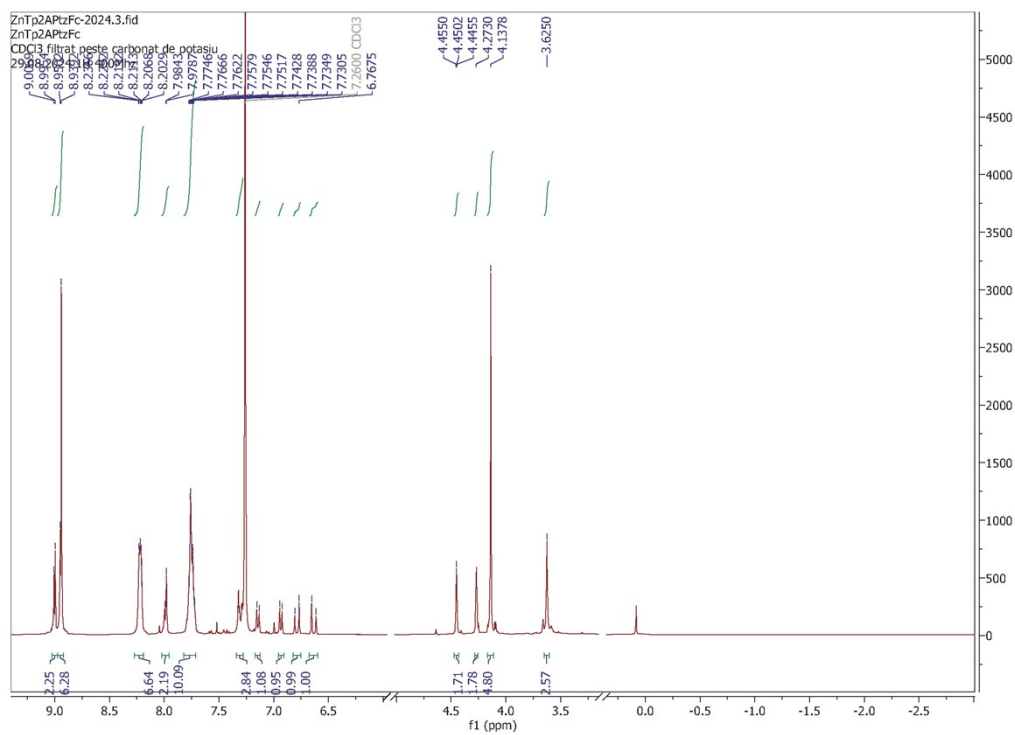


Fig.S12. HRMS (ESI+) of *comp. 4a*



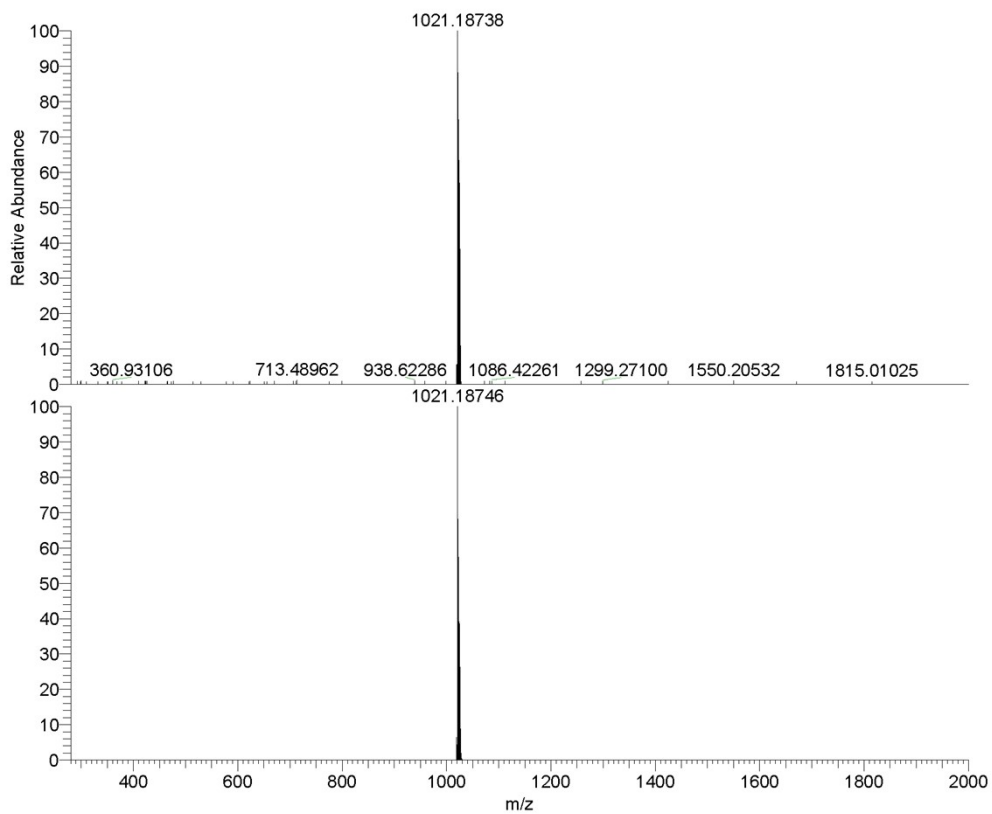


Fig.S15. HRMS (ESI+) of *comp. 4b*

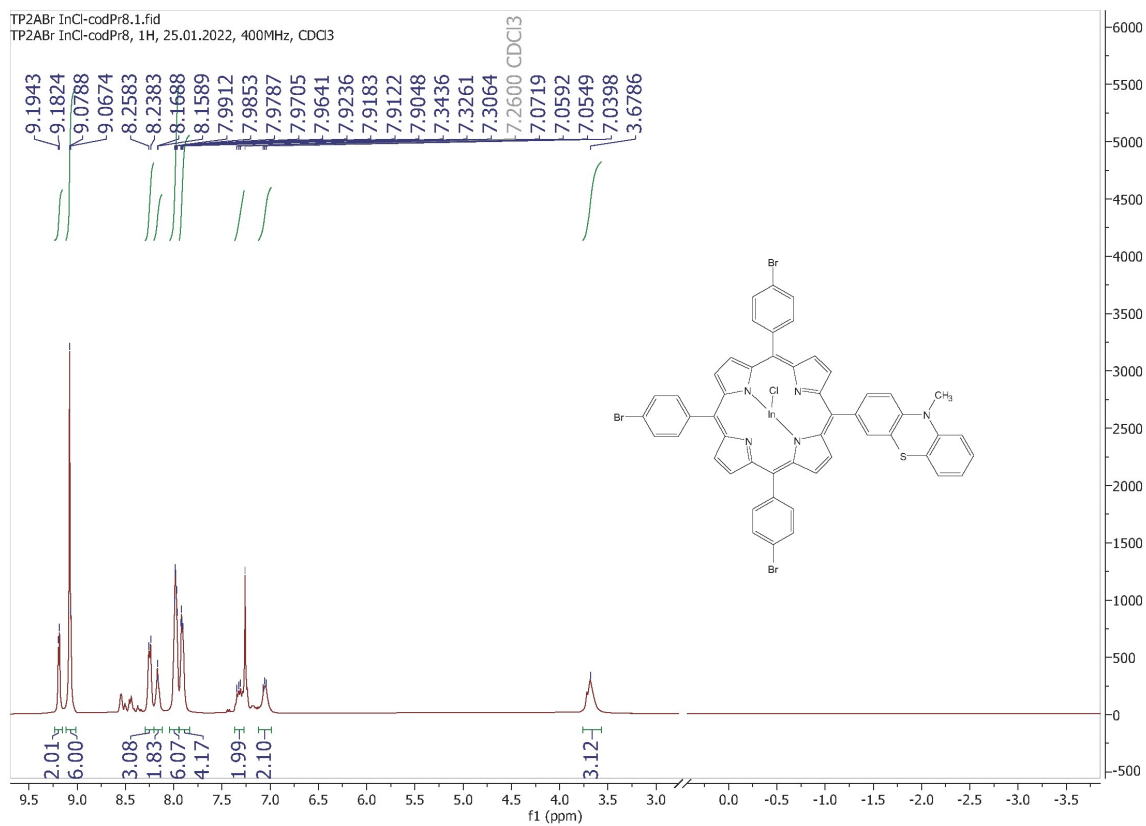


Fig.S16. <sup>1</sup>H NMR of *comp. 5a*, CDCl<sub>3</sub>, 400MHz

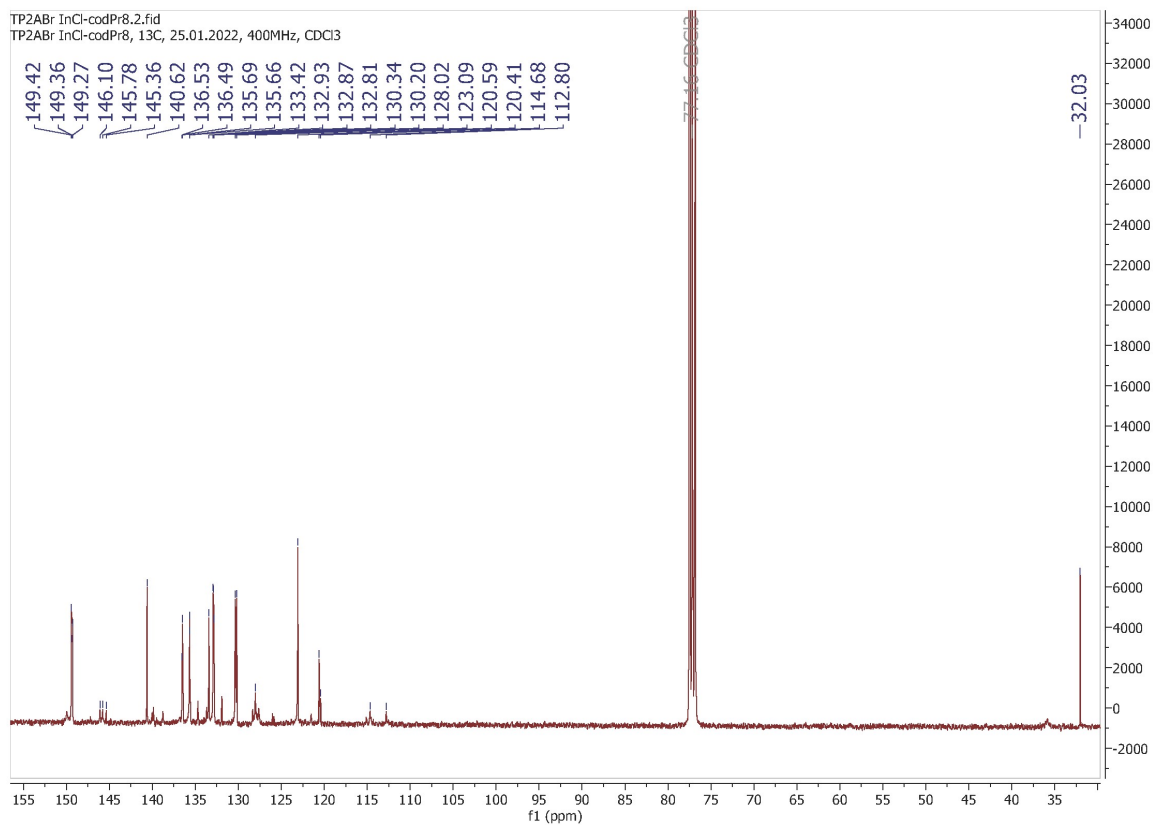


Fig.S17.  $^{13}\text{C}$  NMR of *comp. 5a*,  $\text{CDCl}_3$ , 100MHz

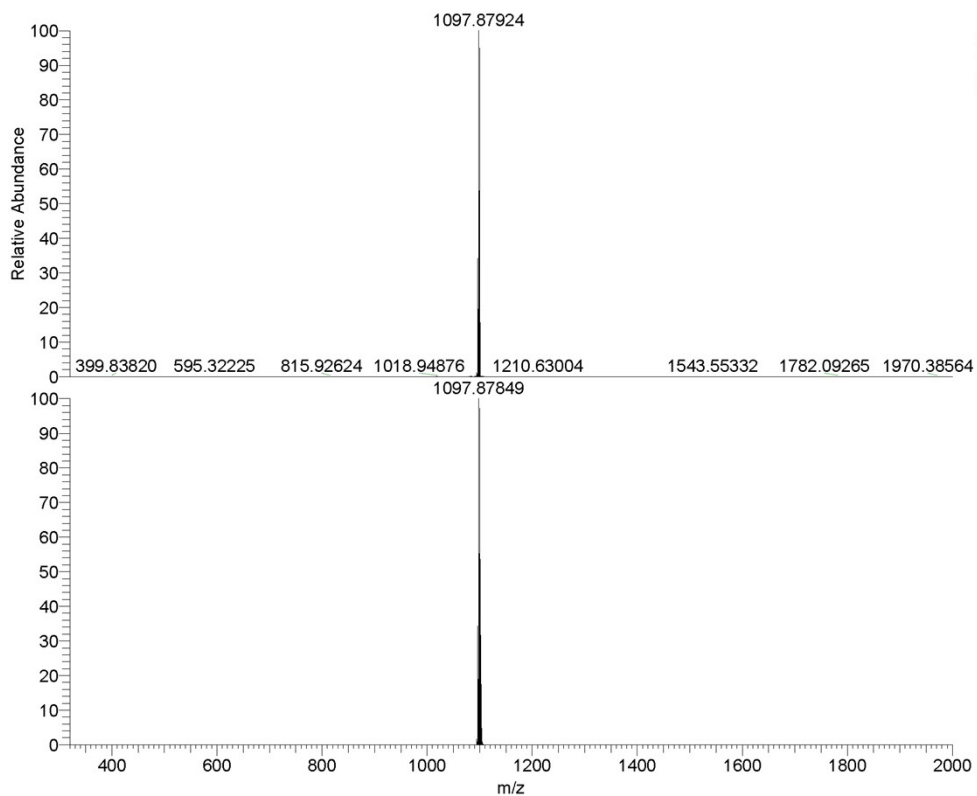
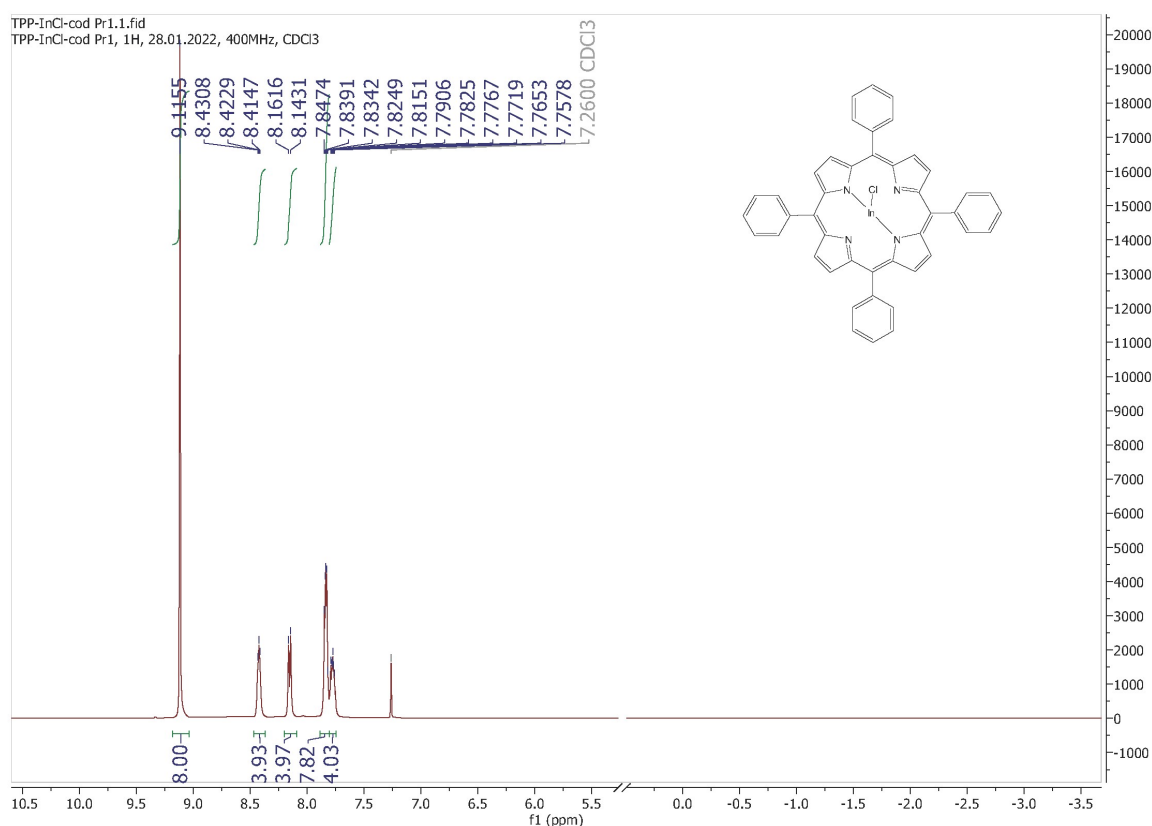


Fig.S18. HRMS (ESI+) of *comp. 5a*

## II. Synthesis of In(III) 5,10,15,20-tetraphenyl porphyrin chloride, *comp. 6a*

5,10,15,20-tetraphenyl porphyrin **6** (1 mmol, 0.614g), InCl<sub>3</sub> (1,4 mmol, 0.31g), and sodium acetate (6.1 mmol, 0.5g) were added to 25 ml of acetic acid. The mixture was refluxed for 8 hours, after which the resulting solution was cooled to room temperature. The precipitate obtained was washed with distilled water and recrystallized from a solvent system comprising CH<sub>2</sub>Cl<sub>2</sub> and heptane (1:1). The compound **6a** was obtained as a purple powder with a yield of 35% (0.27g).

<sup>1</sup>H-NMR (400 MHz, CDCl<sub>3</sub>) δ ppm 9.12 (s, 8H, H<sub>β</sub>), 8.43-8.41 (m, H<sub>Ph</sub>, 4H), 8.15 (d, 4H, H<sub>Ph</sub>, <sup>3</sup>J=7.4 Hz), 7.84-7.81 (m, H<sub>Ph</sub>, 8H), 7.79-7.75 (m, H<sub>Ph</sub>, 4H), <sup>13</sup>C-NMR (100 MHz, CDCl<sub>3</sub>) δ ppm, 121.8, 126.8, 126.9, 132.8, 134.3, 135.1, 141.7, 149.5. Elemental Anal. Calcd. for C<sub>44</sub>H<sub>28</sub>ClIn<sub>4</sub>: C, 69.26; H, 3.70; N, 7.34; Found: C, 69.20, H, 3.68, N, 7.23, HRMS (APCI+) Calc. for C<sub>44</sub>H<sub>29</sub>ClIn<sub>4</sub> [M+H] 763.11140, measured [M+H] 763.11047



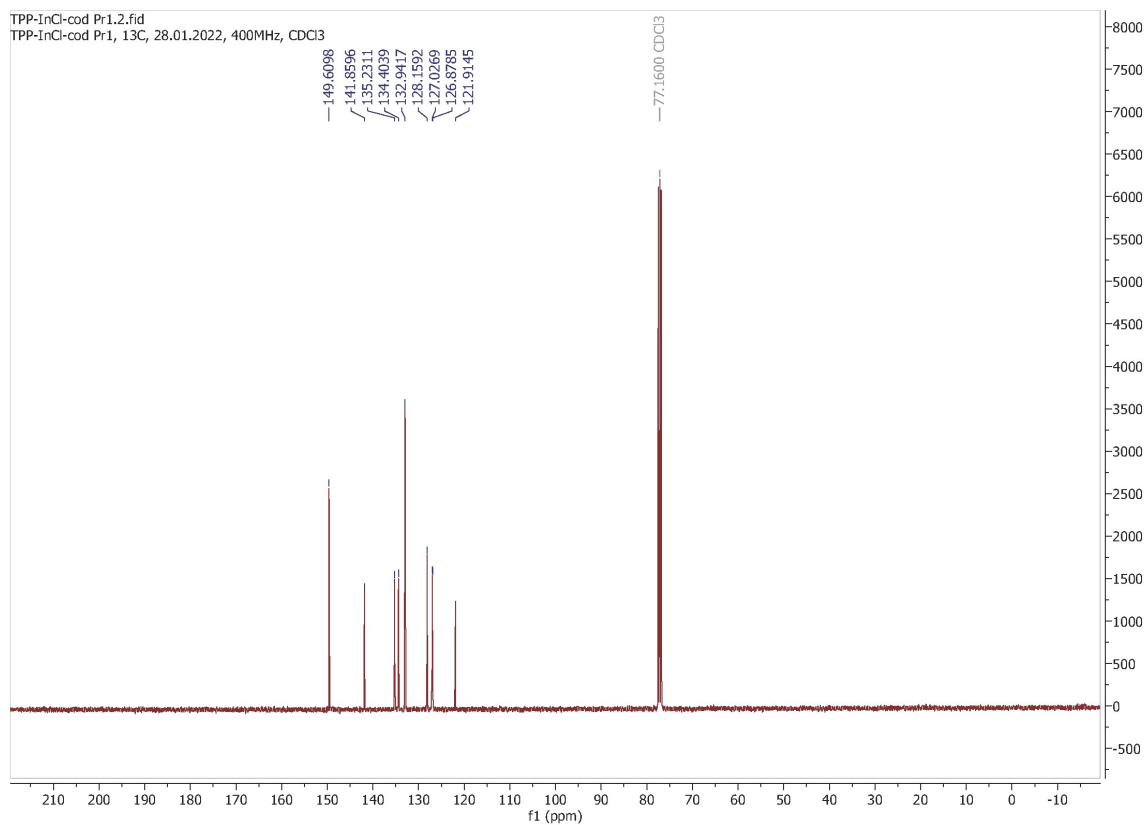


Fig.S20.  $^{13}\text{C}$  NMR of *comp. 6a*,  $\text{CDCl}_3$ , 100MHz

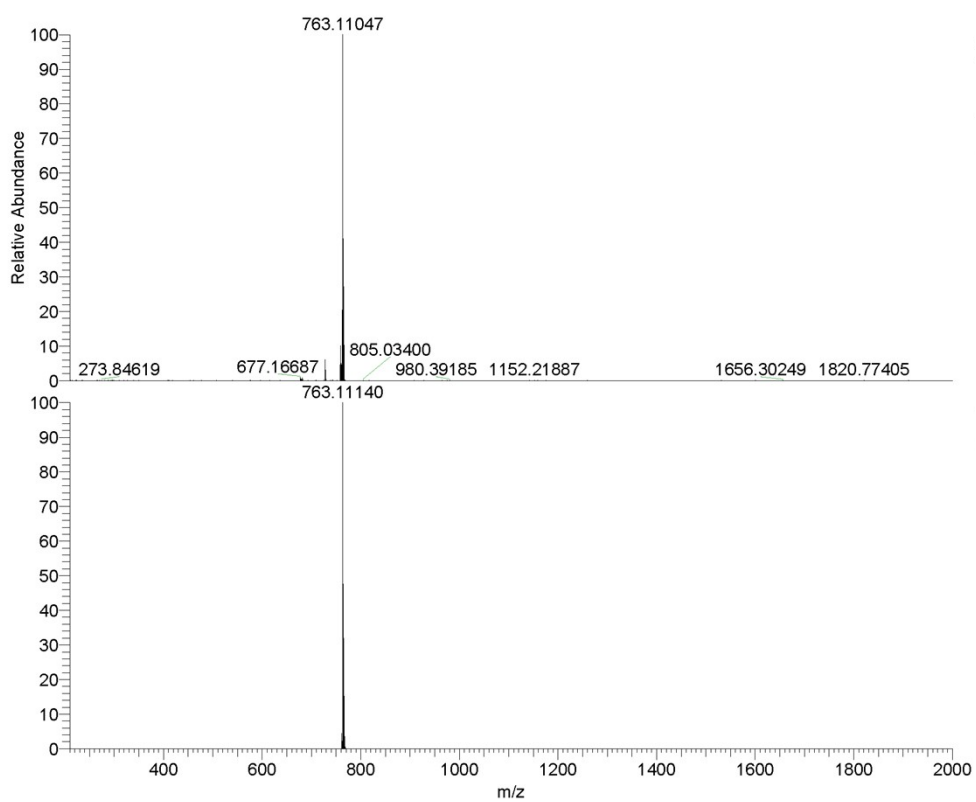


Fig.S21. HRMS (APCI+) of *comp. 6a*

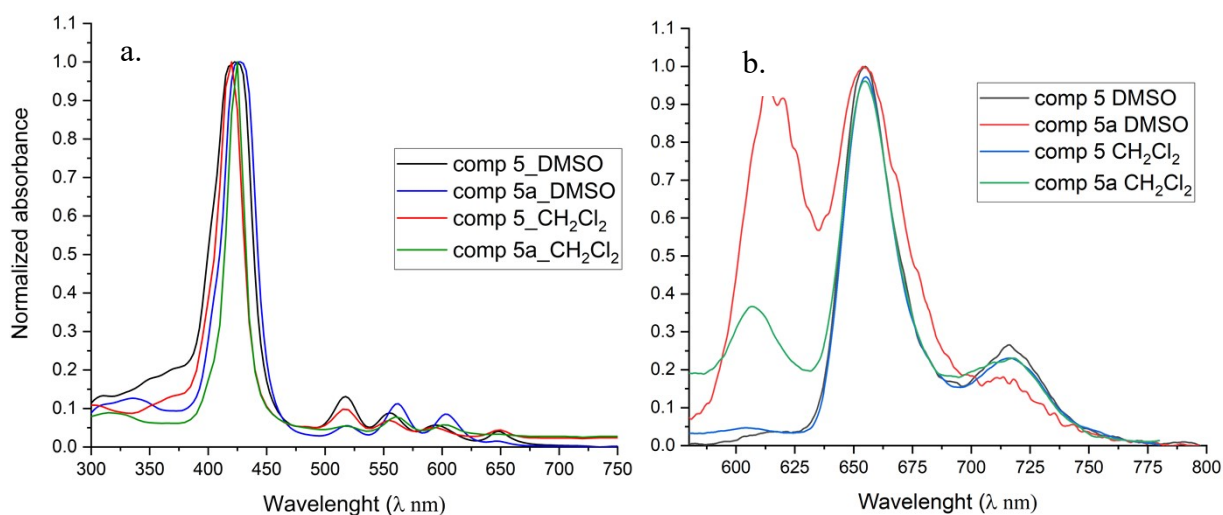


Fig.S22. a) normalized UV-Vis absorbance spectra of comp. **5** and **5a** in DMSO, b) normalized fluorescence emission spectra of comp. **5** and **5a** in DMSO

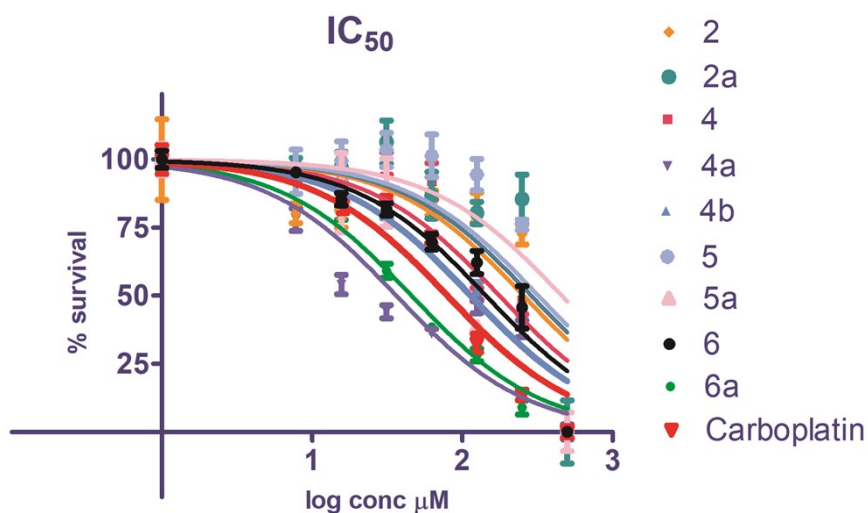


Fig.S23. Sigmoidal dose-response curves resulted from the depiction of survival percents relative to the untreated control (y axis) in relation to the logarithm of the compounds concentration (x axis).

Table S1. The cell survival in A2780 populations treated with sublethal concentration of compounds 2, 2a, 4, 4a, b, 5, 5a, 6, 6a and the effect of photoactivation on treated cells: the hillslope or slope factor generated by linear regression analysis in the 95% confidence interval (best-fit values) quantify the cell growth inhibition in each case.

Compound	Hillslope ±standard deviation	F#	Deviation from 0 p value	Treatment with photoactivation through irradiation	Hillslope ±standard deviation	F#	Deviation from 0 p value
6a	<b>-0.0057</b> ± 0.0015	14.42	0.0067*	PDT-6a	<b>-0.0152</b> ± 0.0019	58.18	0.0001*
4	<b>-0.0033</b> ± 0.0012	7.70	0.0275*	PDT-4	<b>-0.0103</b> ± 0.0021	22.33	0.0021*
4b	<b>-0.0029</b> ± 0.0018	2.47	0.1550	PDT-4b	<b>-0.0048</b> ± 0.0018	7.38	0.0299*
4a	<b>-0.0117</b> ± 0.0018	41.61	0.0004*	PDT-4a	<b>-0.0139</b> ± 0.0024	34.84	0.0006*
2	<b>-0.0051</b> ± 0.0026	3.935	0.0877	PDT-2	<b>-0.0016</b> ± 0.0021	0.59	0.4670
2a	<b>-0.0053</b> ± 0.0025	4.57	0.0698	PDT-2a	<b>-0.0012</b> ± 0.0017	0.48	0.5096
5	<b>-0.0015</b> ± 0.0012	1.59	0.2475	PDT-5	<b>0.0005</b> ± 0.0014	0.12	0.7376
5a	<b>0.0009</b> ± 0.0012	0.55	0.4808	PDT-5a	<b>-0.0038</b> ± 0.0015	6.34	0.0399*
6	<b>-0.0024</b> ± 0.0013	2.94	0.1300	PDT-6	<b>-0.0071</b> ± 0.0018	16.10	0.0051*

# F is the ratio resulted from F test of unequal variance towards a null hypothesis; F indicates the difference from the constant metabolic rate (0% decrease or increase of metabolic rate).

\* significant reduction of the cells metabolic rate in the studied concentration interval, since the hillslope is significantly different from 0

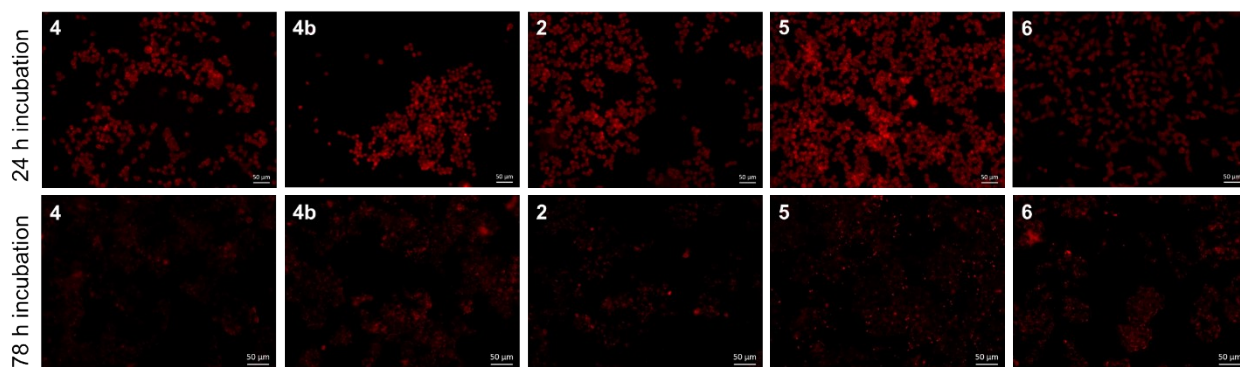


Figure S24. Fluorescence microscopy images of A2780 cells treated with porphyrin derivatives 4, 4b, 2, 5 and 6 at a final concentration of 20 μM under standard cell culture conditions (37°C, 5% CO<sub>2</sub>), incubated for 24 (top) and 72 hours (bottom).

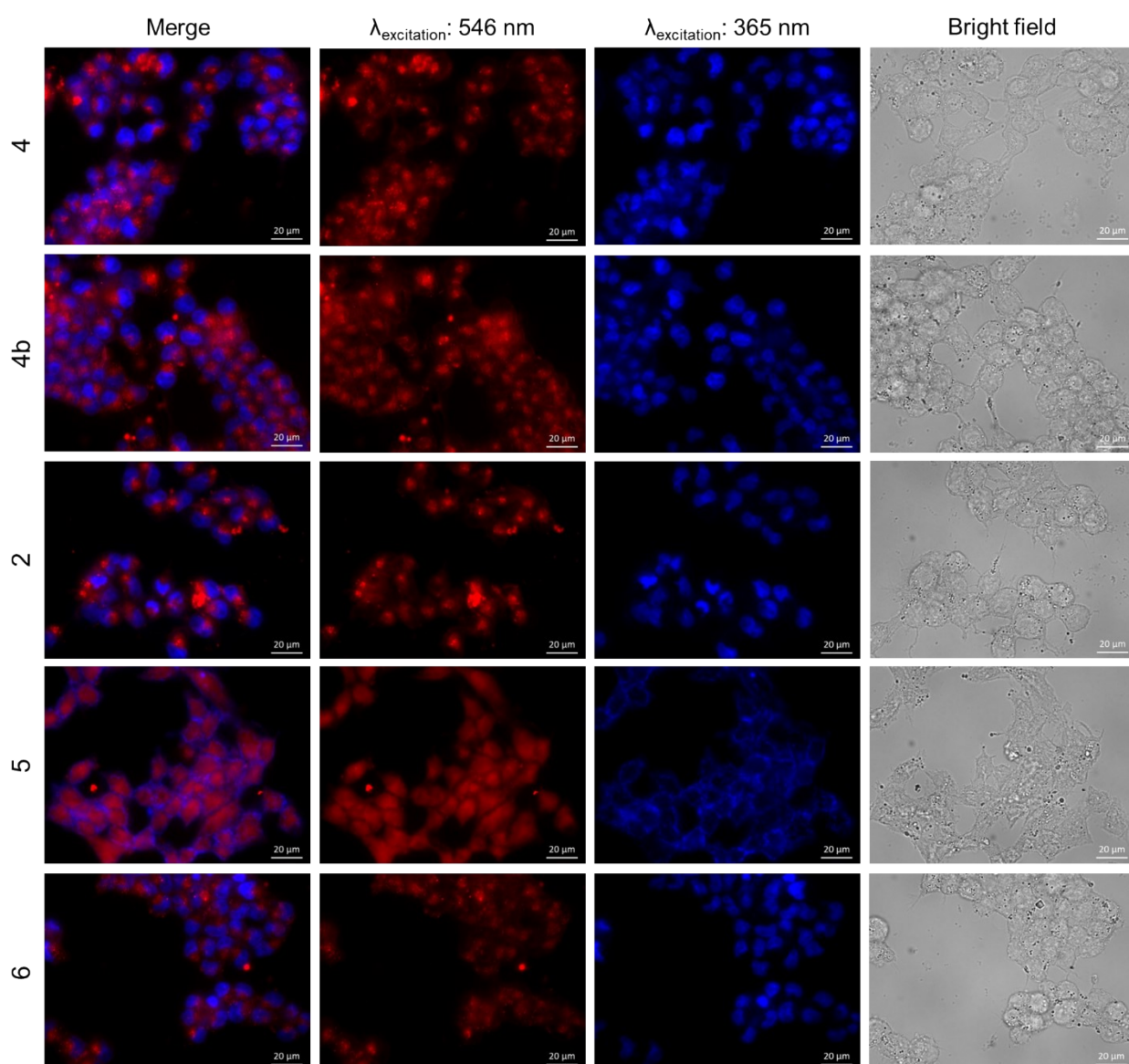


Figure S25. Fluorescence microscopy images of A2780 cells treated with porphyrin derivatives 4, 4b, 2, 5 and 6, in comparison with their corresponding bright field images.

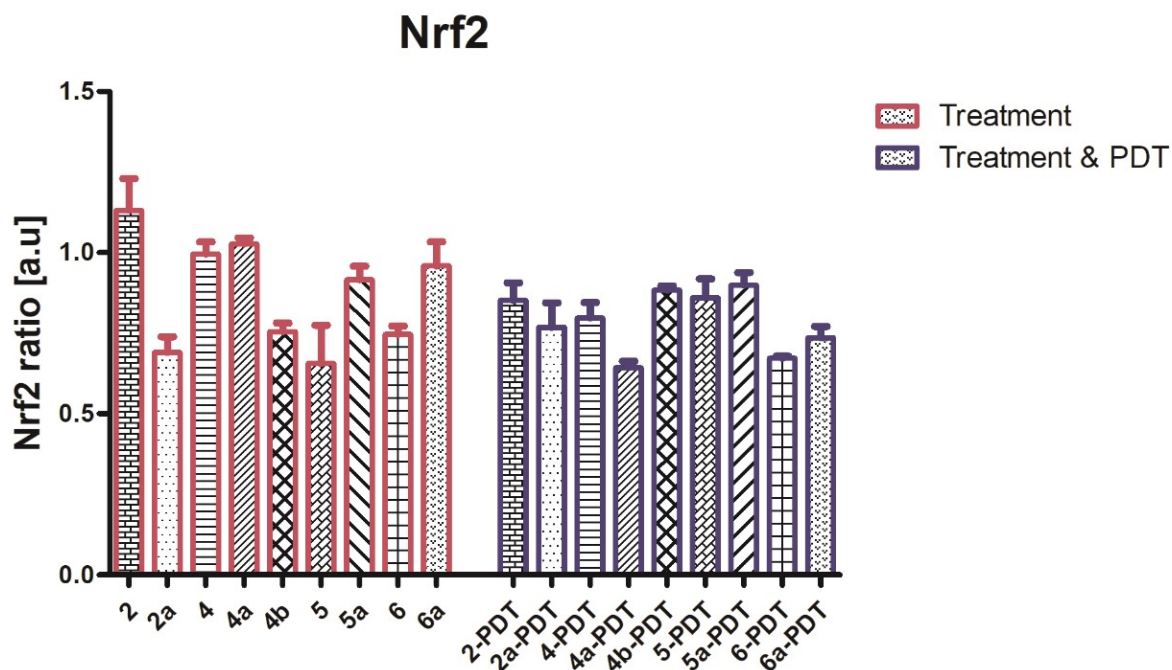
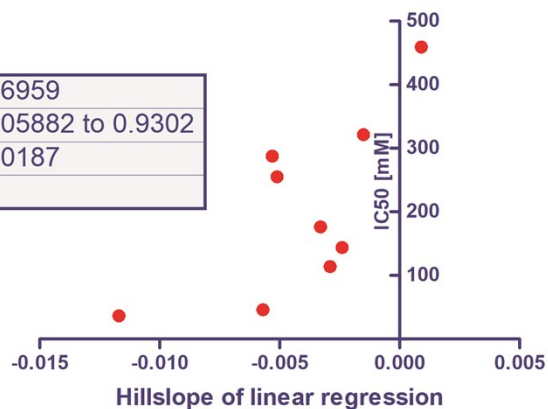


Fig.S26. The level of nuclear factor erythroid 2-related factor 2 (Nrf-2) in A2780 cells subjected to treatment with the sublethal doses of 20 $\mu$ M 2, 2a, 4, 4a,b, 5, 5a, 6a and TPP 6, in the presence or absence of photodynamic therapy. The Nrf2 ratio was calculated against the untreated control Nrf2 values, or against the photoirradiated abbreviated “PDT”, untreated control, respectively.

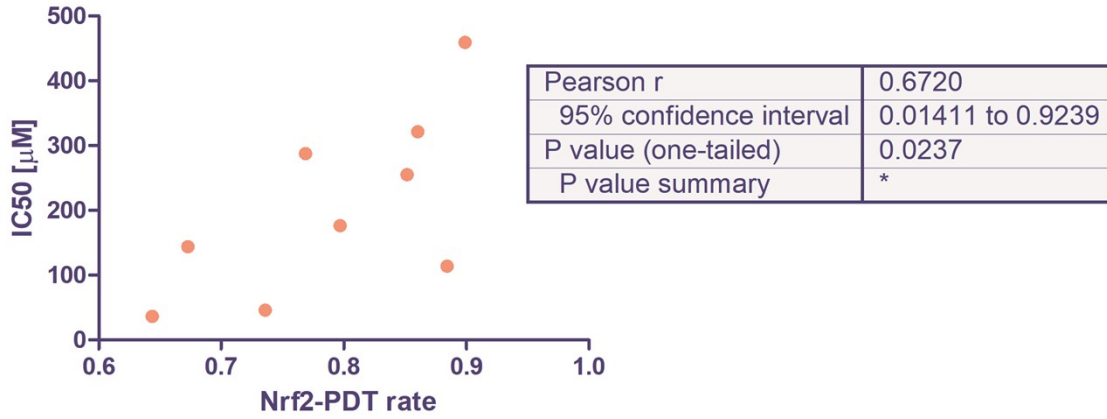
### Correlation between cytotoxicity and metabolic rate

Pearson r	0.6959
95% confidence interval	0.05882 to 0.9302
P value (one-tailed)	0.0187
P value summary	*



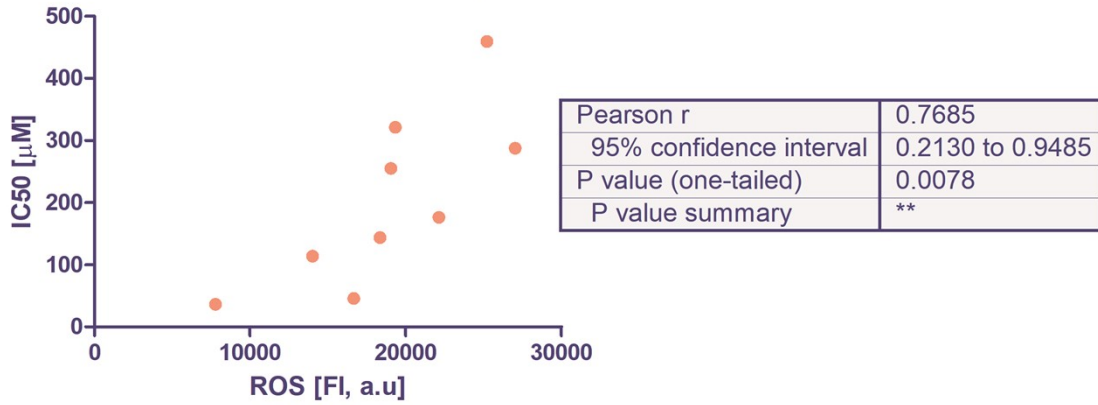
a.)

### Correlation between cytotoxicity and Nrf2-PDT



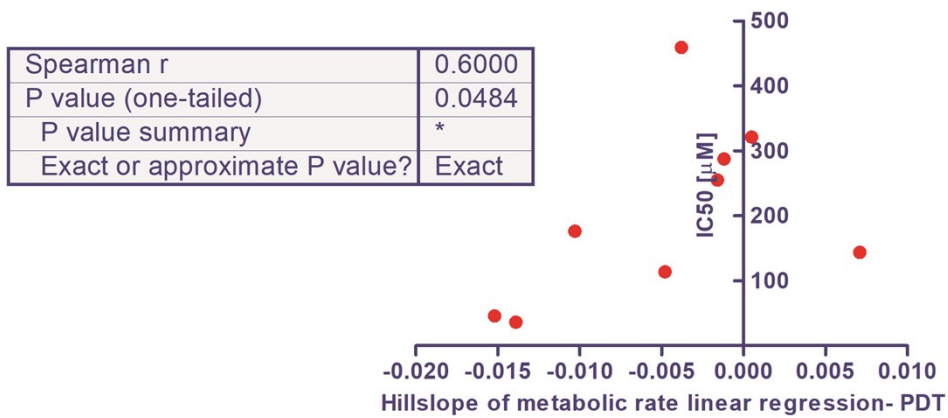
b.)

### Correlation between cytotoxicity and ROS



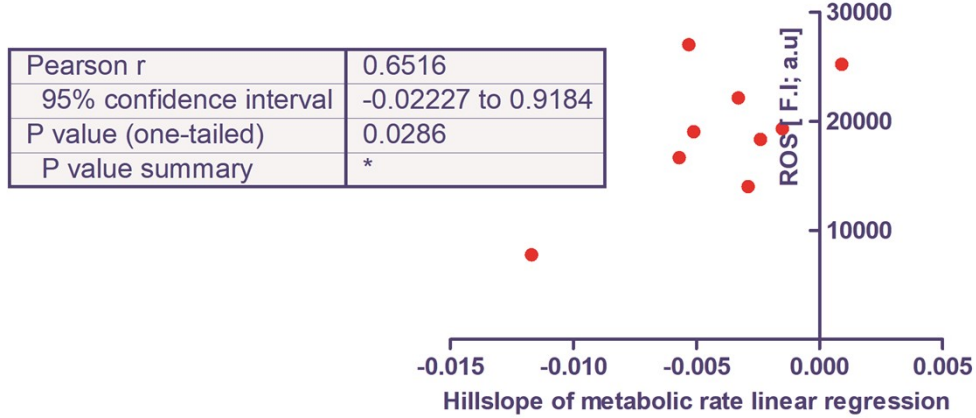
c.)

### Correlation of cytotoxicity and metabolic rate after PDT



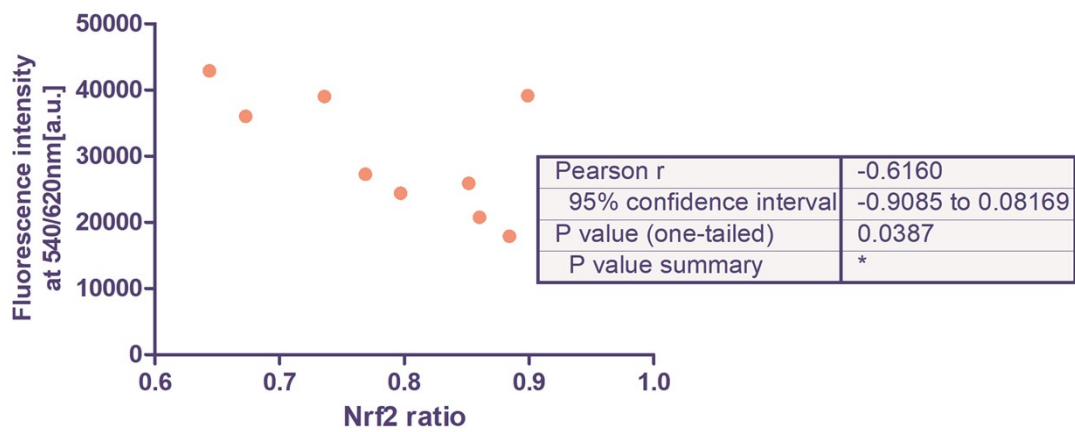
d.)

### Relationship between metabolic rate and ROS level



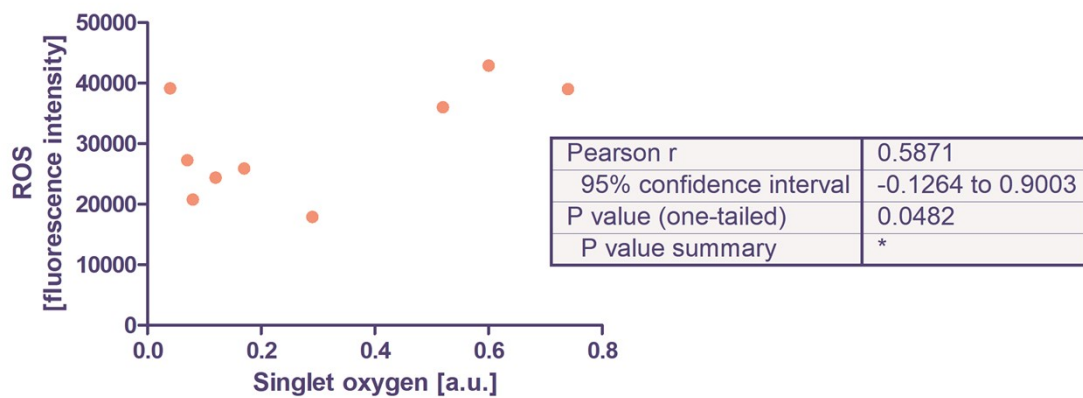
e.)

### Relationship between ROS-PDT and Nrf2-PDT



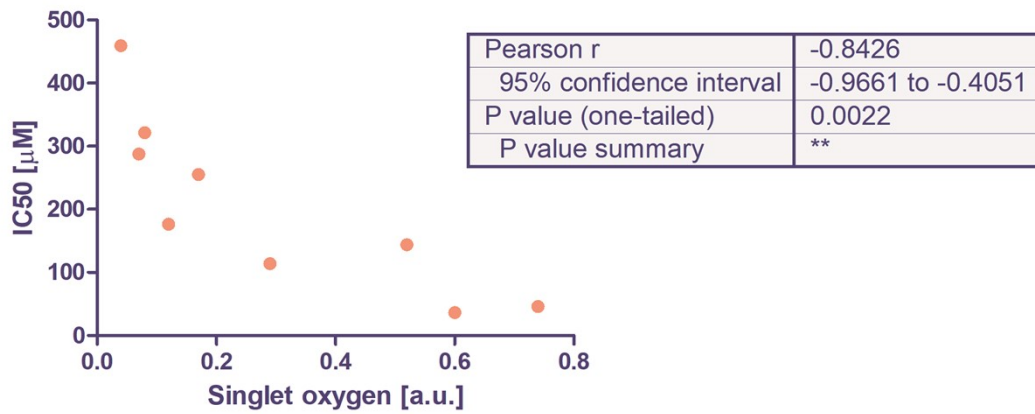
f.)

### Relative singlet oxygen yield vs ROS-PDT



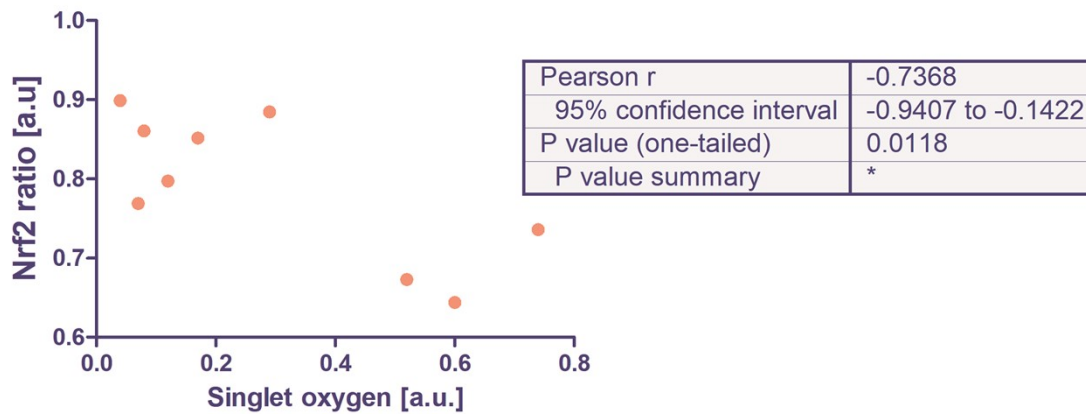
g.)

### Relative singlet oxygen yield vs cytotoxicity



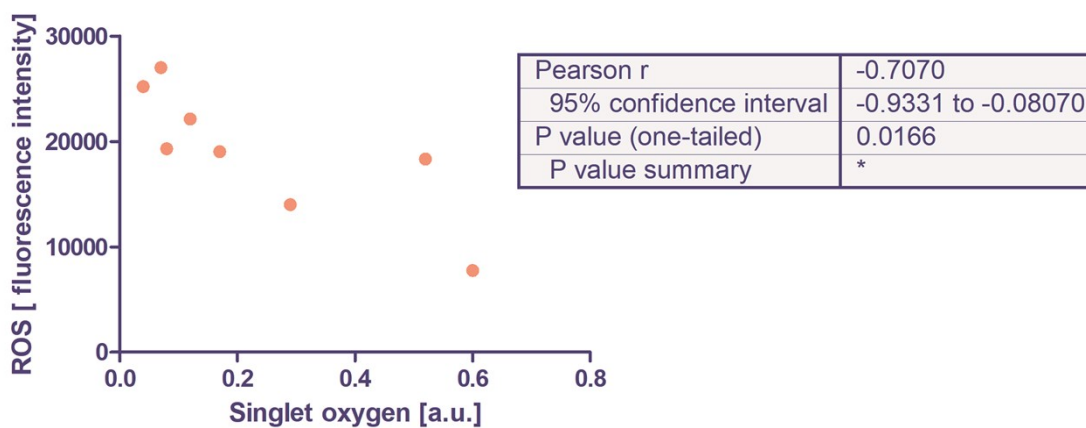
h.)

### Relative singlet oxygen yield vs Nrf2-PDT



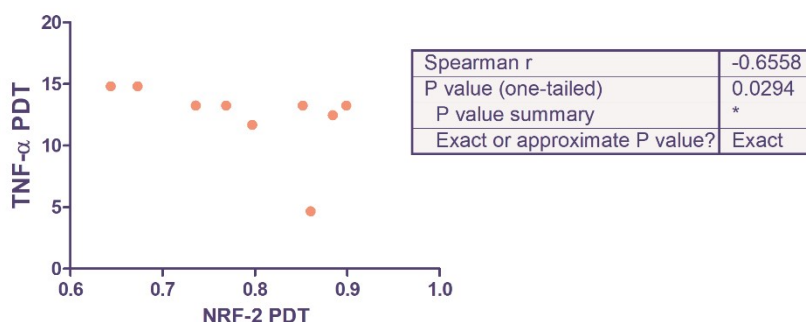
i.)

### Relative singlet oxygen yield vs ROS



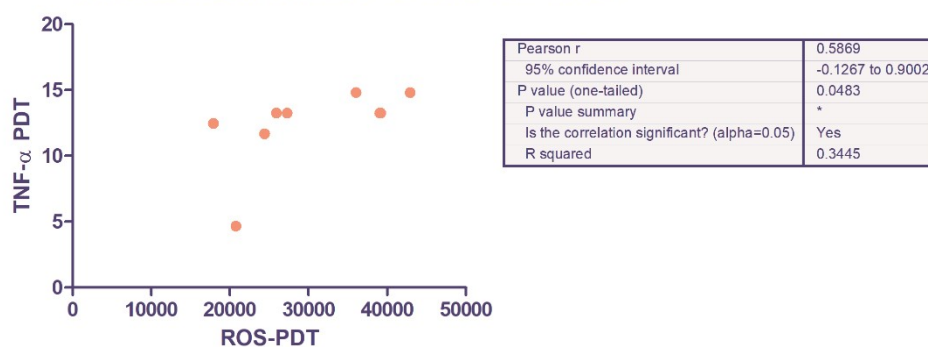
j.)

Correlation between NRF-2 PDT and TNF- $\alpha$  PDT



k.)

Correlation between ROS-PDT and TNF- $\alpha$  PDT



l.)

Fig.S27. a.- 1. Significant correlations between different biologic features: cytotoxicity, metabolic reductive capacity, singlet oxygen quantum yield, reactive oxygen species (ROS) Nrf2 expression and TNF- $\alpha$  following the A2780 cells treatment with 2, 2a, 4, 4a, 4b, 5, 5a, 6a, respectively the cells treatment with 2, 2a, 4, 4a, 4b, 5, 5a, 6a and photoirradiation. The inserted cartridges contain information about the correlation type and parameters; PDT abbreviation refers to the A2780 cells treated as subjected to photoirradiation.

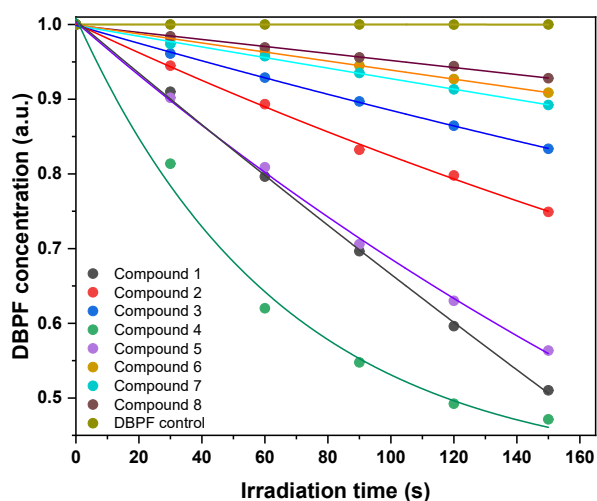


Fig.S28. Normalized spectrum of DBPF sensor degradation in the presence of compounds 2, 2a, 4, 4a, b, 5, 5a, 6, 6a (in DMSO)

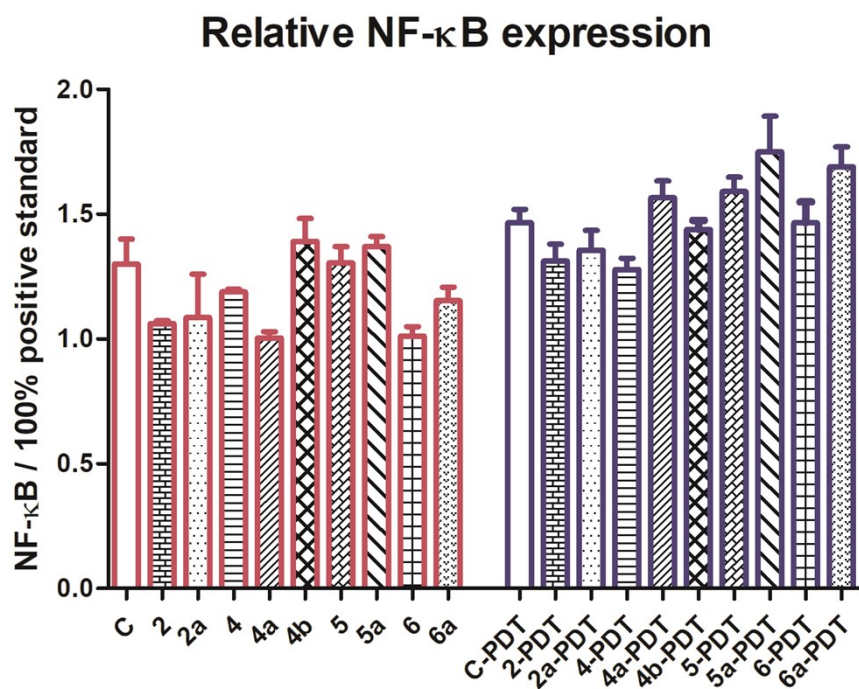
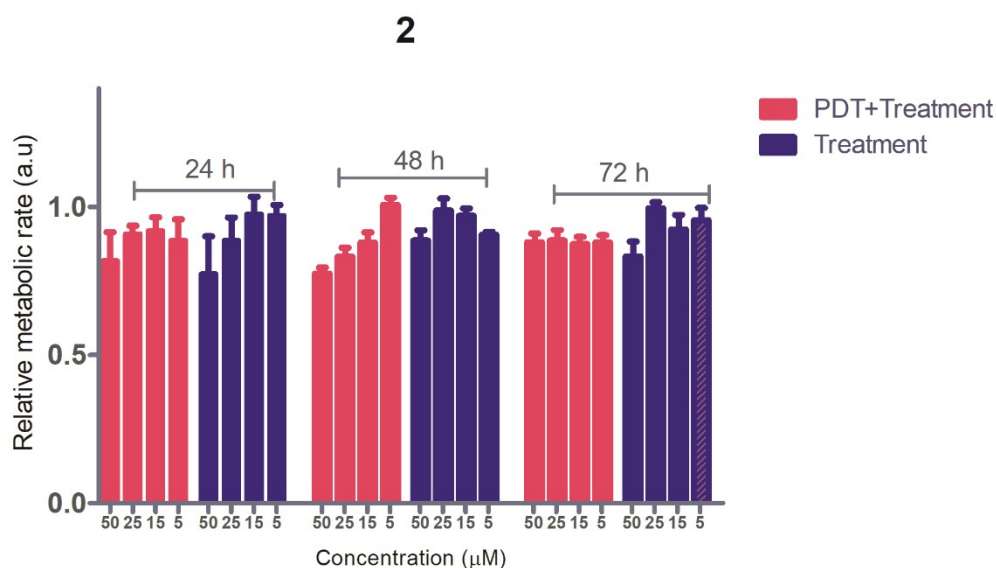
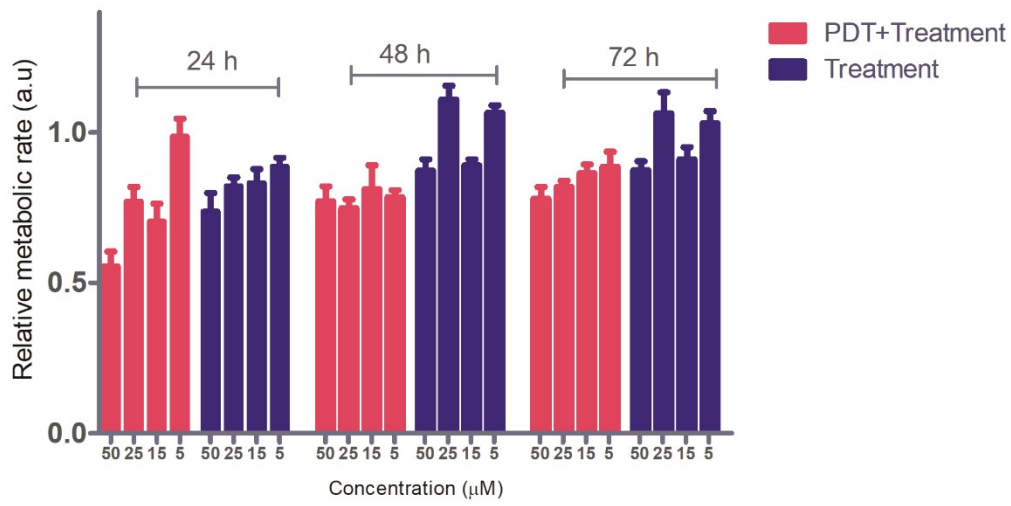


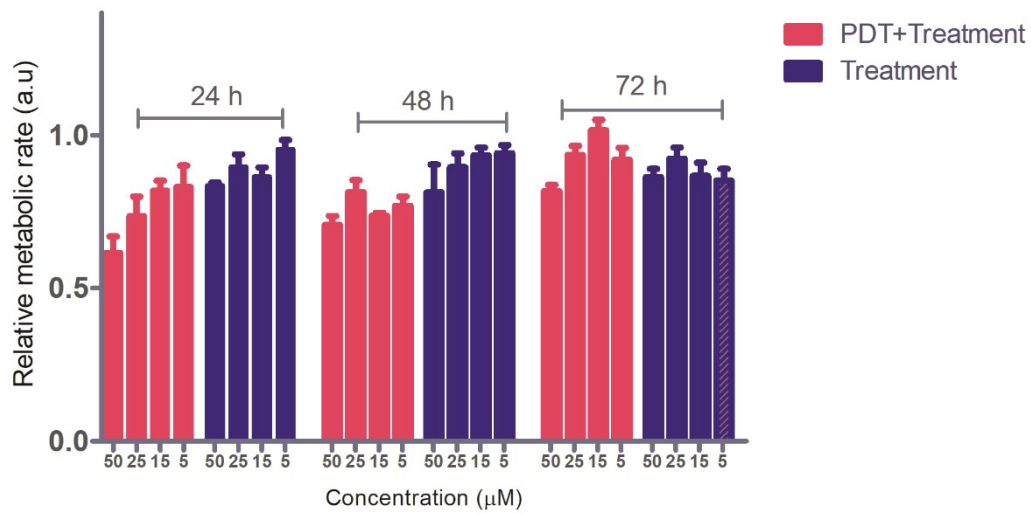
Fig. S29. The level of NF- $\kappa$ B transcription factor in A2780 cells following the 24-hours treatment with 20  $\mu$ M compounds 2, 2a, 4, 4a, b, 5, 5a, 6, 6a and photoirradiation; the values are expressed as relative absorbance versus the absorbance of the highest standard (100%) contained by the assay kit; PDT abbreviation indicates the photoirradiated and treated samples. The changes induced by the treatment, in the presence or absence of irradiation indicates no significant modulation.



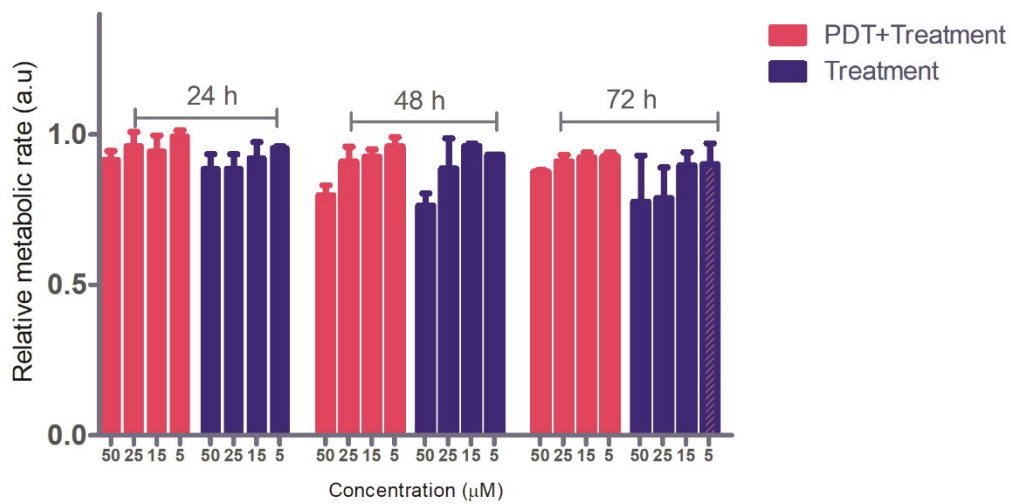
4



4b



5



6

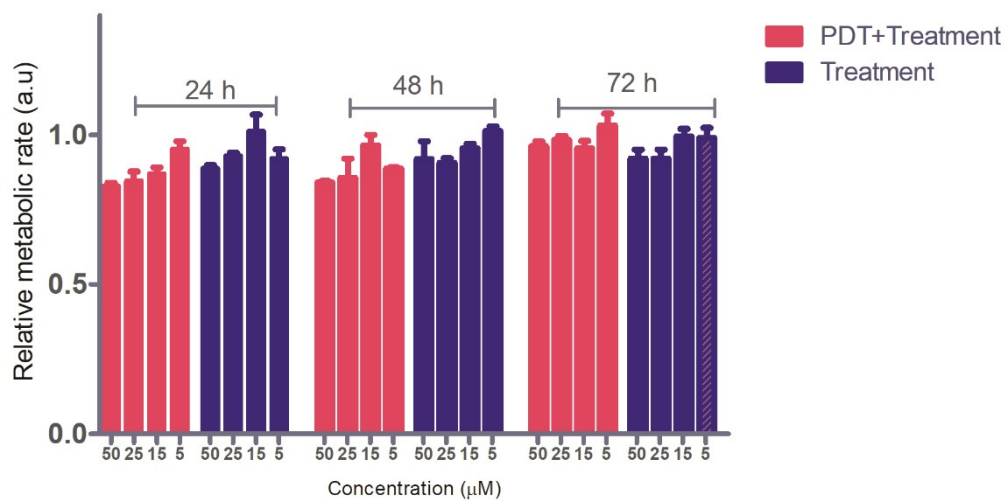


Fig. S30. The metabolic rate modulation in treated A2780 cells, within 72 hours interval, in the presence or absence of photoirradiation (PDT). Compounds 2, 4, 4b, 5 and 6 were assessed at the concentrations of 5; 15; 25 and 50  $\mu\text{M}$ , and the measurements were made at 24, 48 and 72 hours.

---